

The ν EYE Neutrino Telescope:

Conceptual Design Report

Shaomin CHEN ¹, YangHwan Ahn², Davide Franco ³, Fabio Mantovani⁴, Aldo Ianni⁵,
 Jiyong Choi ⁶, S. Gwon ⁶, K. K. Joo ⁷, Chang Hyon Ha ⁸, Kim Siyeon ⁸,
 Jong-Chul Park ⁹, M. Pac, ¹⁰, Pouya Bakhti¹¹, Meshkat Rajaee¹¹, Seodong Shin ^{11,12},
 Young Ju Ko ¹³, Bo-Young Han ¹⁴, Jihoon Choi ¹⁵, B. R. Ko ¹⁶, HyangKyu
 Park ¹⁶, Gihan Hong ¹⁷, Jaebak Kim ¹⁷, Minseo Kim¹⁷, Kyungmin Lee ¹⁷, E.
 Won ¹⁷, Jae Hyeok Yoo ¹⁷, J.Y. Cho ¹⁸, J.Y. Lee ¹⁸, D.W. Jeong ¹⁸, H.J. Kim ¹⁸,
 Sin Kyu Kang ¹⁹, Myung-Ki Cheoun ²⁰, V. Kornoukhov ²¹, V. Kobychev ²²,
 V.I. Tretyak ^{22,23}, Steve Elliott ²⁴, Jose R. Alonso ²⁵, Janet M. Conrad ²⁵, Michael
 H. Shaevitz ²⁶, Joshua Spitz ²⁷, and Daniel Winklehner ²⁵

¹Center for High Energy Physics Department of Engineering Physics Tsinghua
 University, Beijing, China

²Institute of Particle and Nuclear Physics, Henan Normal University, Xinxiang, Henan,
 China

³APC, Université Paris Cité, CNRS, Astroparticule et Cosmologie, Paris, France

⁴Department of Physics and Earth Sciences University of Ferrara Polo Scientifico e
 Tecnologico, Ferrara, Italy

⁵I.N.F.N. Laboratori Nazionali del Gran Sasso, Assergi (AQ), Italy

⁶Center for Precision Neutrino Research, Chonnam National University, Republic of
 Korea

⁷Physics Department, Chonnam National University, Republic of Korea

⁸Department of Physics, Chung-Ang University, Seoul, Republic of Korea

⁹Department of Physics, Chungnam National University, Korea

¹⁰Department of Radiology, Dongshin University, Naju-si, Korea

¹¹Laboratory for Symmetry and Structure of the Universe, Department of Physics,
Jeonbuk National University, Jeonju, Korea

¹²Center for Theoretical Physics of the Universe, Institute for Basic Science, Daejeon,
Korea

¹³Department of Physics, Jeju National University, Jeju, Korea

¹⁴Korea Atomic Energy Research Institute Daejeon, Republic of Korea

¹⁵Korea Astronomy and Space Science Institute, Yuseong-gu, Daejeon, Republic of Korea

¹⁶Accelerator Science Department, Korea University Sejong Campus, Republic of Korea
¹⁷Korea University, Physics Department, Republic of Korea

¹⁸Kyungpook National University, Republic of Korea

¹⁹School of Liberal Arts, Seoul National University of Science and Technology, Republic
of Korea

²⁰Soongsil University, Physics Department, Republic of Korea

²¹National Research Nuclear University MEPhI: Moscow, Russia

²²Institute for Nuclear Research of NASU, Kyiv, Ukraine

²³Institute of Experimental and Applied Physics, CTU Prague, Prague, Czech Republic

²⁴Los Alamos National Laboratory, Los Alamos, United States

²⁵Laboratory for Nuclear Science, Massachusetts Institute of Technology, Cambridge,
MA, USA

²⁶Department of Physics, Columbia University, New York, NY, United States

²⁷Physics Department, University of Michigan, Ann Arbor, MI, United States

January 21, 2026

Abstract

The **ν EYE** (“new eye”, Neutrino Experiment at YEmilab, nuEYE.korea.ac.kr) neutrino project leverages the existing large pit at Yemilab located in South Korea, to reveal the

existence of sterile neutrino, the up-turn of the neutrinos from the Sun, and the first minimum of the neutrino oscillation over distances on the order of tens of kilometers for the first time. This initiative is expected to facilitate a wide range of significant scientific and technological advancements within both South Korean and international communities engaged in neutrino science and technology. The **ν EYE** aims to investigate the largely unexplored sector of almost-massless lepton in the elementary particle physics in detail. The emphasis will be placed on the study of real time nuclear processes and reactions involving possible sterile neutrinos on timescales down to nanoseconds in ultra-high intense or radioactive neutrino beams for the first time in the world; the **ν EYE** looks at to-be universal oscillation (“up-turn” in the electron neutrino survival probability) of neutrinos predicted by the three neutrino oscillation paradigm. This will confirm or deny our current understanding on the particle interactions of the lepton sector; and measurement of the first oscillation minimum between the first and second neutrinos in mass.

- Prepared by the **ν EYE** proto-collaboration.

Contents

1 The νEYE Project Executive Summary	5
2 Introduction	7
3 Detailed Plan of Research and International Collaboration	9
3.1 Sterile neutrino search program	9
3.1.1 Current status of sterile ν search	9
3.1.2 Sterile ν search in the ν EYE experiment	10
3.2 BSM searches with the IsoDAR accelerator	14
3.3 Solar science with neutrinos	16
3.4 Reactor neutrino program	20
3.5 Geoneutrinos and astronomical sources	21
3.6 Neutrinoless double beta decay	23
3.7 Detector	24
3.7.1 The ν EYE detector	24
3.7.2 One-Tonne Prototype Detector	28
3.7.3 Slow LS	32
3.7.4 Photodetector	37
3.7.5 Environmental Backgrounds	40
3.8 R&D on next generation neutrino detector	42
3.8.1 Water based LS	42
3.8.2 Opaque LS	43
3.8.3 Others	44
3.9 International collaboration	44
4 Construction and Utilization Plan	45
5 Plan to Organize Research Groups	45
6 Expected Research Outcome	46
7 Implementation Plan by Phase and a Cost Estimate	47
7.1 Implementation plan	47

1 The ν EYE Project Executive Summary

The **ν EYE** (“new eye”, Neutrino Experiment at YEmilab, nuEYE.korea.ac.kr) neutrino project leverages the existing large pit at Yemilab located in South Korea, to reveal the existence of sterile neutrino, the up-turn of the neutrinos from the Sun, and the first minimum of the neutrino oscillation over distances on the order of tens of kilometers for the first time. This initiative is expected to facilitate a wide range of significant scientific and technological advancements within both South Korean and international communities engaged in neutrino science and technology.

The **ν EYE** aims to investigate the largely unexplored sector of almost-massless lepton in the elementary particle physics in detail. The emphasis will be placed on

- the study of real time nuclear processes and reactions involving possible sterile neutrinos on timescales down to nanoseconds in ultra-high intense or radioactive neutrino beams for the first time in the world;
- the **ν EYE** looks at to-be universal oscillation (“up-turn” in the electron neutrino survival probability) of neutrinos predicted by the three neutrino oscillation paradigm. This will confirm or deny our current understanding on the particle interactions of the lepton sector; and
- Measurement of the first oscillation minimum between the first and second neutrinos in mass.

The major scientific themes outlined above represent significant questions that warrant further exploration.

The **ν EYE** facility is proposed to be constructed in the “Liquid Scintillator Counter” (LSC) hall with a ultra high-intensity accelerator based neutrino beam facility and/or high radioactive source. Adjacent to the LSC hall, a highly sophisticated radio-purification facility will be built to provide the radio-purified scintillator and water to the **ν EYE** experiment.

Key international collaborations have been developed with the United States IsoDAR team (MIT, Michigan), and European team for the detector construction (INFN, APC).

2 Introduction

Curiosity about nature and the universe has led to enormous advancements in science and technology throughout human history. Today, fields such as physics, mathematics, chemistry, and life science are highly advanced and complex, providing significant technological benefits to humanity. From particle physics to cosmology, we study objects in the universe on scales ranging from the smallest particles to the largest cosmic structures, all based on first principles.

Understanding the nature of interactions among fundamental particles at the smallest scale has been the primary interest in particle physics. This interest has resulted in what we now call the Standard Model (SM) of particle physics, which has been experimentally and theoretically developed and validated since the last century. Nevertheless, there are compelling reasons to believe that the SM is not the ultimate model of nature at the most miniature scale. One very relevant example of this proposal is the non-zero neutrino mass.

The existence of a hypothetical new neutrino may explain the finite neutrino mass. Studies of the Sun's metallicity with neutrinos are crucial in astrophysics. The ordering of the neutrino mass, and the nature of neutrinos as leptons (Dirac vs. Majorana), and CP violation are of great interest. This proposal will discuss some of the most outstanding physics programs.



Figure 1: A picture of a large Yemilab hall, courtesy of Dr. K. S. Park. Similar one can also be seen from [Nature 30 May, 2024](#).

Yemilab is a new underground laboratory located in Korea at a depth of 1,000 m (<https://arxiv.org/abs/2402.13708>). Yemilab includes a cylindrical pit with 19.5 m in diameter and 22 m in height, designed as a multipurpose laboratory for next-generation experiments, as shown in Fig. 1. At this site, our proposed **ν EYE** (Neutrino Experiment at YEmilab) detector is planned to be installed through this proposal. Here the **ν EYE** detector refers to a proposed $\mathcal{O}(2)$ -kilo tonne liquid scintillator detector that will be described in detail in the following sections. First, we discuss the physics programs with the **ν EYE** detector, and later, we discuss the status as well as the plan for the international collaboration.

Further information about **ν EYE** can be found on its website at nuEYE.korea.ac.kr.

3 Detailed Plan of Research and International Collaboration

3.1 Sterile neutrino search program

In the neutrino sector, the SM of particle physics requires extension to account for the observed neutrino oscillations, which imply nonzero neutrino masses. Further extensions may involve one or more sterile neutrinos (ν_s) to explain experimental anomalies observed over the past few decades.

3.1.1 Current status of sterile ν search

The first experimental anomaly, indicating a possible sterile neutrino signal was reported by the LSND experiment more than 20 years ago [PRD 64 112007 \(2001\)](#), reporting an excess of $87.9 \pm 22.4 \pm 6.0$ events in $\bar{\nu}_\mu \rightarrow \bar{\nu}_e$ appearance search. Utilizing a neutron spallation facility, the KARMEN experiment did not confirm [PRD 65 112001, \(2002\)](#) this observation, but couldn't entirely exclude it. The MiniBooNE $\bar{\nu}_e + \nu_e$ combined [PRL 129 201801 \(2022\)](#) is compatible with LSND but the low energy spectrum has excess. However, the μ BooNE result [PRL 130 011801 \(2023\)](#) disfavors MiniBooNE and LSND but does not rule out these results completely. Recent μ BooNE result [Nature volume 648, 64–69 \(2025\)](#) disfavors a single sterile neutrino state.

In nuclear-reactor-based $\bar{\nu}_e$ disappearance experiments, there have been extensive searches for sterile neutrinos. The Daya Bay and RENO experiments found a rate deficit but it is more likely that the flux calculation needs to be revised. NEOS, STEREO, PROSPECT, DANSS, SOLID, and Neutrino4 studied the neutrino spectrum with near and far detectors for the flux-independent oscillation study. Most experiments saw no evidence, except that Neutrino4 reported an arguable 3σ signal with $\Delta m^2 = 7 \text{ eV}^2$ [PLB 829, 137054, \(2022\)](#).

The SAGE and GALLEX experiments, solar ν_e disappearance experiments with the radiochemical extraction of ^{71}Ge indicated so-called the Gallium anomaly [PRD 97, 073001 \(2018\)](#). Most recently, the BEST experiment, which used a 3.4 MCi ^{51}Cr radioactive neutrino source with the radiochemical extraction method, revealed the 4σ deviation consistent with $\nu_e \rightarrow \nu_s$ oscillations [PRC 105, 065502 \(2022\)](#).

Having a consistent picture in current sterile neutrino search experiments is somewhat tricky. In particular, it is increasingly important to carefully examine the BEST result, which uses the same neutrino source but real-time neutrino detection as an independent cross-check.

3.1.2 Sterile ν search in the ν EYE experiment

• **High-intensity accelerator (IsoDAR)**

The ν EYE detector's combination of low energy threshold and large-size is unmatched by any above-ground detector for electroweak physics. Events in a detector such as ν EYE would be swamped by cosmic-ray backgrounds, hence must be constructed underground. Experiments at accelerators, which are constructed on the Earth's surface, must make use of detectors with smaller footprints and higher energy thresholds to reduce the cosmic-ray background. They also make use of "beam compression" — delivering high intensity beam in short bursts — which adds expense to an accelerator.

Most underground laboratories cannot easily be retrofitted to allow an accelerator to be constructed underground. But because ν EYE is being constructed in an entirely new laboratory, this is the opportunity to re-think the paradigm. This is the concept behind the isotope decay-at-rest (IsoDAR) system — a novel compact cyclotron accelerator and target system that is proposed for installation in an existing tunnel adjacent to ν EYE ([arxiv:2404.06281](https://arxiv.org/abs/2404.06281), [PRD 105 052009, 2022](#)). With this integration, ν EYE will become the first underground accelerator-based experiment, thus advancing the frontiers of rare event searches.

In the US, the IsoDAR antineutrino source is being designed and proposed to the US government. The 60 MeV protons from IsoDAR impinge on a ${}^9\text{Be}$ target, resulting in a high flux neutrons. The neutrons then enter a surrounding ${}^7\text{Li}$ sleeve and produce ${}^8\text{Li}$ via neutron capture, resulting in ${}^8\text{Li} \rightarrow {}^8\text{Be} + e^- + \bar{\nu}_e$. The IsoDAR source can produce 1.67×10^6 IBD events and 7000 $\bar{\nu}_e e^- \rightarrow \bar{\nu}_e e^-$ elastic scattering (ES) events with the ν EYE detector during 5 calendar years of operation. This allows one to search for oscillations associated with one or more sterile neutrinos with higher sensitivity than that with the radioactive sources in the higher Δm^2 region if the design current of 10 mA is reached. This can be seen in Fig. 2. The US group intends to place the IsoDAR accelerator in Yemilab and a proposal is planned to be submitted along with this

proposal. A horizontally long tunnel next to the ν YEYE hall is already placed for the IsoDAR accelerator complex. Given that Yemilab already has an accelerator tunnel to house the IsoDAR accelerator system, we have regularly discussions with a part of the IsoDAR collaboration from MIT and U. of Michigan about future possibilities. A sensitivity figure provided from IsoDAR collaboration is shown in Fig. 2 where five year running is assumed.

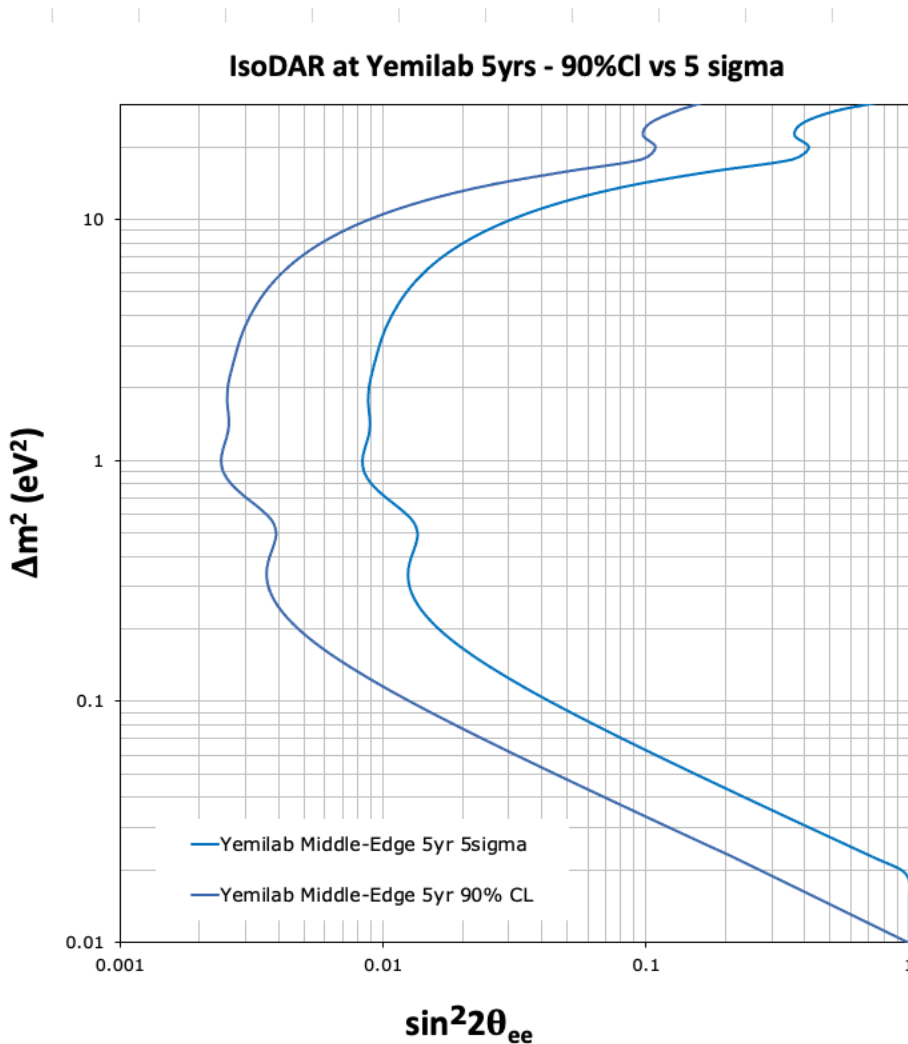


Figure 2: Estimated sensitivities for five year running of IsoDAR are shown. Both 5σ and 90% CL sensitivities are shown.

- **Radioactive source**

Here, we propose a sterile neutrino search program with radioactive neutrino sources, directly measuring the inverse beta decay (IBD) or $\nu_e e^-$ scattering with the **ν EYE** detector. This approach avoids complicated radiochemical processes and instead detects neutrinos in real time. At this stage, we consider two sources; ^{144}Ce and/or ^{51}Cr . The ^{144}Ce produces $\bar{\nu}_e$ via radioactive beta decays and ^{51}Cr produces ν_e via nuclear electron capture. Note that ^{144}Ce is obtained from the nuclear spent fuel, whereas ^{51}Cr is obtained by activating enriched ^{50}Cr with thermal neutrons inside reactors. Therefore, it is relatively easier to prepare ^{51}Cr than ^{144}Ce source. Additionally, 3.4 MCi ^{51}Cr has been used in the BEST experiment but $\mathcal{O}(100)$ kCi ^{144}Ce source has never been produced yet, with an attempt by the SOX experiment, [PRL 107 201801 \(2011\)](#). Note that in fact the neutrinos above the IBD threshold come from the daughter product of ^{144}Ce as indicated in Fig. 3. Also, neutrino energies from ^{51}Cr are also indicated (from [IAEA](#)).

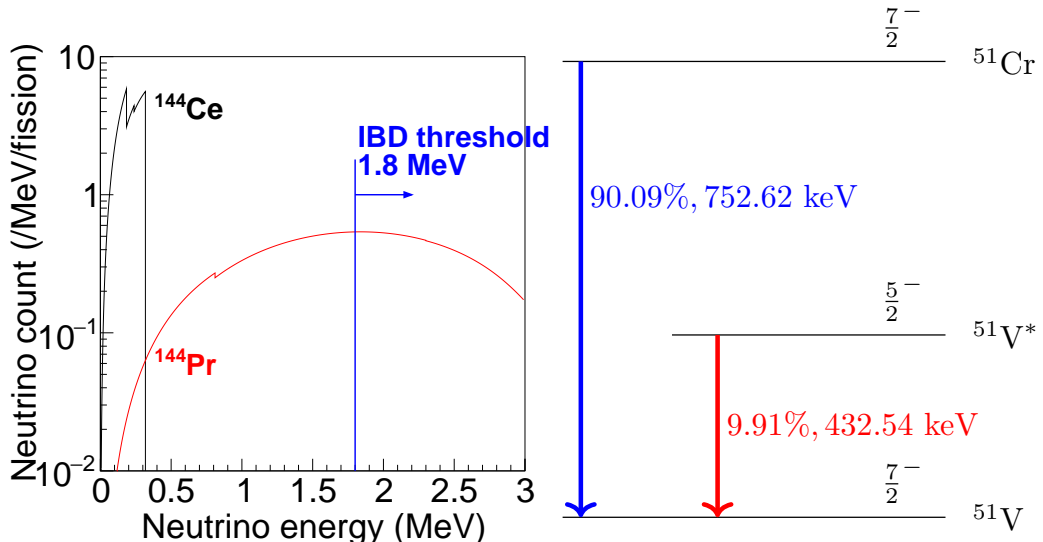


Figure 3: Left: energy distributions of $\bar{\nu}_e$ from β^- decays of ^{144}Ce and ^{144}Pr . Right: a simplified decay transitions of ^{51}Cr with released energies of ν_e .

	^{144}Ce	^{51}Cr
Assumed Activity	100 kCi	10 MCi
Detection Methods	IBD	$\nu_e e^-$ scattering
Half-life	285 days	27.7 days
Expected events (1 yr)	34,000	28,000

Table 1: Comparison between two sources. For expected events, a two-kilo-tonne liquid scintillator detector is assumed.

We estimate the sensitivity with ^{144}Ce in Δm^2 and $\sin^2 2\theta$ for the sterile neutrino search. For that purpose, the **νEYE** detector is assumed. The detailed design parameters of the detector will be addressed later. Sensitivities for source position are shown in Fig. 4. We emphasize here that the primary physics goal in this case is to confirm or rule out the BEST positive signal, which utilized a radioactive source with the radiochemical extraction of the signal. The black curve in Fig. 4 represents the combined limits from experiments with different systematic effect. The key point here is that we propose the IBD or elastic scattering processes for the detection, allowing real-time measurements. Note also that ^{51}Cr with parameters in Table 1 provides essentially similar sensitivity.

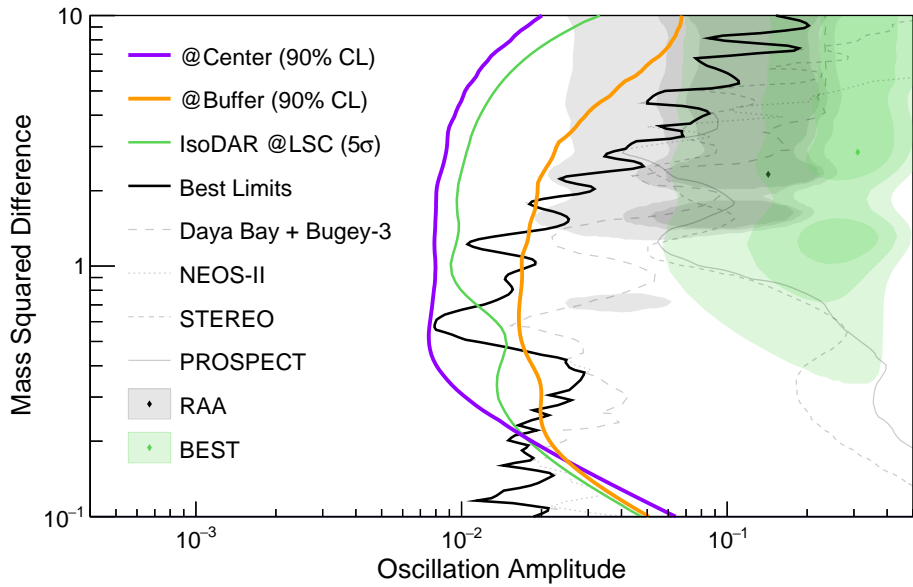


Figure 4: Comparison of sensitivity for source position. The purple and orange curves represent the case where the source is located at the center $(0, 0, 0)$ m and side $(9, 0, 0)$ m of the detector, respectively, with the source activity of 200 kCi and the uncertainty in the radioactivity of 2%. The thick black curve shows the best limit by combining four results (gray curves) shown together. Limits from other experiments are also indicated.

3.2 BSM searches with the IsoDAR accelerator

Since IsoDAR@ **ν EYE** is a first-of-its-kind, the physics program is still under development, but is clearly already rich. The areas that can be explored are identified as international priorities, including Neutrino Properties, Cosmic Connections, and Rare Events. The searches for new physics in each area are expected to have order of magnitude jumps in sensitivity. This is what can be achieved with the incredibly powerful and unprecedented combination of a kiloton-scale, precision and low-background detector and nearly 10^{25} protons on target with an accelerator nearby. The investigation into this physics utilizes two types of particle sources: the “direct flux” of electron antineutrinos from ${}^8\text{Li}$ decay in the IsoDAR source that traverse the **ν EYE** detector, and “indirect sources,” which consist of gammas and neutrons contained within the IsoDAR target but that may subsequently produce Beyond SM particles capable of passing through the source shielding, enter **ν EYE**, and either interact or decay. With its extensive size and uniquely protected environment, **ν EYE** can reconstruct the electrons, photons, and protons that are predicted to result from such signal particle creation inside the detector.

IsoDAR@ **ν EYE** will deliver an extensive program of neutrino property studies. A discussion of the very high sensitivity to oscillations to sterile neutrinos using $\bar{\nu}_e + p \rightarrow e^+ + n$, the inverse beta decay (IBD) interaction, can be found in Sec. 3.1. As another example of compelling new physics searches, IsoDAR@ **ν EYE** will acquire 7000 electron antineutrino elastic scattering (ES) events—the world’s largest sample. Both rate and energy dependence of ES are precisely predicted within the Standard Model (SM) from LEP and LHC data ([PTEP 083C01 \(2020\)](#)). The 1.67 million IBD events determine the normalization, reducing uncertainties, allowing IsoDAR@ **ν EYE** to measure $\sin^2 \theta_W$ with a precision of 1.9% at low Q^2 , more than five times better than reactor experiments. Because of the precise predicted energy dependence of the ES sample, **ν EYE** can also perform a precise phenomenological search for non-standard neutrino interactions (NSIs) involving lepton-lepton couplings, complementing the lepton-quark coupling searches by the active, global coherent neutrino-nucleus scattering program.

With $\bar{\nu}_e e^-$ ES, one can measure the weak mixing angle at around $Q = 6$ MeV a region where no prior measurements exist. This allows us to look for beyond the standard model physics for the first time in this kinematic range, via so called non-standard neutrino interactions ([PRD](#)

[89 072010 \(2014\)](#)). Additionally, IsoDAR facilitates searches for new particles produced in the target and sleeve that decay to $\nu_e\bar{\nu}_e$. The theoretical motivation arises from generally called *light particles* which refer to low-mass mediators of new interactions in the BSM. The **ν EYE** experiment will be most sensitive in the mass range up to $10 \text{ MeV}/c^2$ ([PRD 105 052009, 2022](#)). Once realized, this will be the first facility combining ultra-low background large detector with a high-power accelerator underground in the world.

ν EYE’s antineutrino program also allows searches for Dark Matter, which remains unexplained despite extensive search efforts over the years. A flaw in the approach may be that experiments have predominantly focused on a single type of dark matter, while the truth may be a combination of sources. For example, a fraction of the dark matter may consist of particles exhibit stronger interactions within SM than those predicted by Weekly Interacting Massive Particles (WIMPs) of comparable mass. Such a particle would be slowed down by interactions with the material in the atmosphere and the Earth before reaching our WIMP detectors underground. However, IsoDAR’s intense underground antineutrino beam can enhance this ambient dark matter population through upscattering processes, allowing potential observation in **ν EYE** ([PRD 106 035011 \(2022\)](#)). Additionally, it is plausible that dark matter includes axion-like particles as part of its composition. Axions can be produced through mixing with monoenergetic photons produced by nuclear excitations in the IsoDAR target, traverse the shielding, and decay or interact in the **ν EYE** detector ([PRD 107 095010 \(2023\)](#)).

A wide range of cosmological questions are addressed by introducing a dark sector. Neutron–dark sector couplings are also motivated by the neutron beam/bottle experiment lifetime discrepancy ([Ann. Rev. Nucl. Part. Sci. 55 27 \(2005\)](#), [PRL 111 222501 \(2013\)](#), [PRC 97 055503 \(2018\)](#), [PRL 127 162501 \(2021\)](#)). Such couplings would allow neutrons to disappear from the target and reemerge in **ν EYE**’s central and far side through $n \rightarrow n' \rightarrow n$ transitions, and the underground, ultra-large design of **ν EYE** allows for much higher sensitivity than surface experiments ([PRD 107 075034 \(2023\)](#)). Alternatively, if the n' are Majorana, then $n \rightarrow n' \rightarrow \bar{n}$ may occur, depositing $\sim 2 \text{ GeV}$ of energy in the **ν EYE** upon annihilation. This is a B violating effect with implications for conditions in the early universe ([EPJC 81 33 \(2021\)](#)).

This is only a subset of the well-motivated theoretical questions that **ν EYE** will be able to ad-

dress. However, because IsoDAR@ **ν EYE** is first-of-its-kind, it also opens search opportunities that are entirely motivated by the experimental design. An example is a search for $X \rightarrow \nu_e \bar{\nu}_e$, where the new particle, X is produced by mixing with the monoenergetic photons and the $\bar{\nu}_e$ interacts via IBD interactions, producing sharp peaks (PRD 105 052009 (2022)). No past detector has been able to perform such a search before because it requires the unique underground environment and enormous size of **ν EYE**, coupled with a neutrino source such as IsoDAR. If such an effect were seen, it would transform theoretical physics.

3.3 Solar science with neutrinos

The Borexino experiment has significantly advanced recent measurements of solar neutrinos. The most recent key findings include a measurement of neutrino flux from the CNO cycle of $6.7^{+1.2}_{-0.8} \times 10^8 \text{ cm}^{-2} \text{ s}^{-1}$ (PRD 108 102005 2023) and the measurement of *pp*–chain solar neutrinos at $6.1 \pm 0.5^{+0.3}_{-0.5} \times 10^{10} \text{ cm}^{-2} \text{ s}^{-1}$ (Nature 562, 505 2018). With this and the ^7Be , *pep*, and ^8B results, the MSW-LMA prediction is favored; however, it still carries significant uncertainties that necessitate more precise measurements to investigate neutrino interactions beyond SM. The **ν EYE** experiment aims to achieve this challenging goal.

One important unresolved question in solar science pertains to the metallicity of the Sun, which refers to the abundance of elements with $Z > 2$. Various analyses of spectroscopic data yield divergent results (“High or low” metallicity, A&A 661 A140 2022, A&A 653 A141 2021). The solar neutrino fluxes, particularly those produced by reactions within the CNO cycles, can address this issue and the latest data prefer the high metallicity model, but with significant uncertainty. The **ν EYE** experiment will provide a clear resolution to this critical issue with high statistics (see Fig. 5) in an exceptionally radio-pure environment.

We will examine the vacuum-MSW transition region of the electron neutrino survival probability previously explored by Borexino (Nature 562, 505 2018), by conducting precision measurements of ^7Be , *pep*, and ^8B solar neutrinos to either confirm or refute the current understanding of the neutrino oscillation phenomena. This will also allow for an investigation of neutrino interactions within the context of Beyond SM physics.

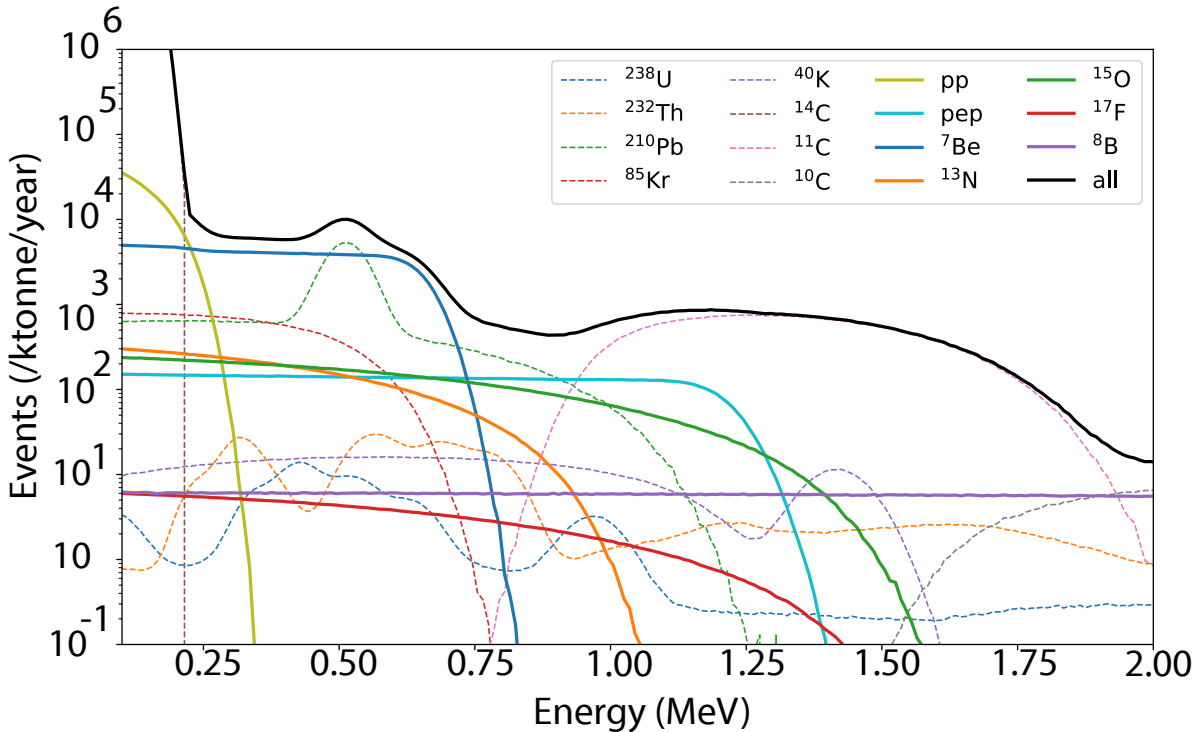


Figure 5: Expected neutrinos from the Sun and from background radioactive sources as a function of the electron kinetic energy in the ν EYE detector are shown. Here, we assume B16-GS98 model for the solar neutrino flux calculation ([J. Phys. Conf. Ser. 1056 012058 2018](#)), $^{14}\text{C}/^{12}\text{C} = 2 \times 10^{-18}$, and the energy resolution of $5\%/\sqrt{E(\text{MeV})}$ at the Yemilab site.

Here we show the recent compilation of the ν_e survival probability as a function of the neutrino energy measured by Borexino (black dots with error bars, [Nature 562, 505 2018](#)), in Fig. 6, along with expectations from the ν EYE experiment, which assumes a similar period of data taking but a target volume five times larger. There is significant improvements in ^7Be and *pep* neutrino measurements as shown in Fig. 6. Note that two points next to ^8B represent the ν EYE experiment's expectations in the [3-5] MeV and [5-10] MeV energy bins. If we further increase the statistics, we may be able to see the up-turn in the MSW-LMA solution.

For this, we relied on the statistical uncertainty of the Borexino results and scaled it down according to the expected statistics of the ν EYE experiment. These expectations may be over-simplified for *pp* neutrino, where pile-up from ^{14}C is expected to be serious. The frequency of n pile-up in a certain time window Δt for an activity f is $e^{-f\Delta t}(f\Delta t)^{n-1}/(n-1)!$ from Poisson statistics ([arxiv:2303.08512](#)). The expected rates for *pp* solar neutrino, as well as the single and

double rates for ^{14}C decays are summarized in Table 2.

	pp	^{14}C (single)	^{14}C (double)
Rates	400 (cpd)	687 Hz	0.236 Hz

Table 2: Expected rates for pp solar neutrino in counts per day (cpd), single and double rates for ^{14}C decays for a 2 kilo-tonne detector of 5-year running period. The concentration of $^{14}\text{C}/^{12}\text{C} = 2 \times 10^{-18}$ g/g is assumed.

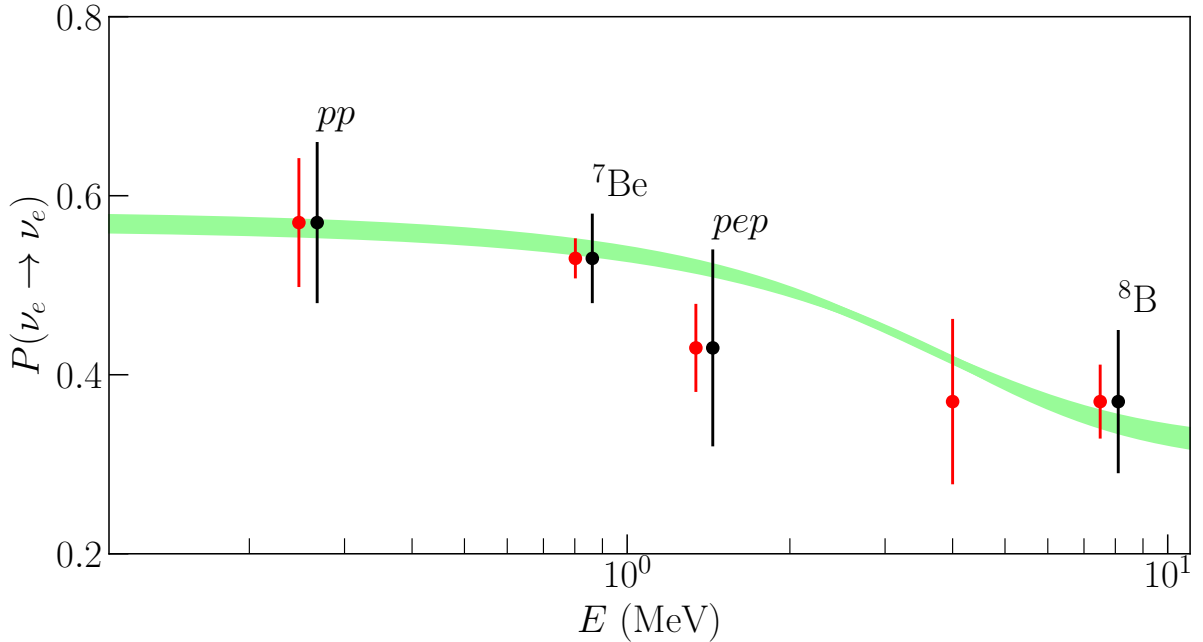


Figure 6: Black dots with error bars show a compilation of the ν_e survival probability as a function of the neutrino energy measured by Borexino. The red dots with error bars are expectations from the **νEYE** experiment, shifted left a bit from Borexino central values, assuming a similar running period. The green curve represents the theoretical prediction ([JHEP 11,004, 2003](#)) with **PDG** values of θ_{12} and Δm_{21}^2 , where its finite thickness reflects their uncertainties. Two points next to ^8B represents the **νEYE** experiment's expectation in the [3,5] MeV and [5,10] MeV bins.

There is a statistical effect of this pile-up for the pp solar neutrino measurement. From fits using the **νEYE** detector simulation that includes pile-up from ^{14}C , we found that the statistical uncertainty does not scale with $1/\sqrt{N}$ where N is the fit yield of the pp neutrino due to the pile-up. This is reflected in Fig. 6, which shows only a 20% reduction in statistical uncertainty (instead of the expected 55%). However, with longer data collection and pile-up removal using the detector directionality, we expect significant improvements beyond this simulation stage.

Two issues need to be addressed to achieve significantly more precise solar neutrino measurements. Since these measurements suffer predominantly from background neutrinos produced by radioactive isotope decays (See Fig. 5), an extremely pure radio purification process must first be applied. Here we assume the concentration of $^{14}\text{C}/^{12}\text{C} = 2 \times 10^{-18}$ g/g (PLB 422 349 1998) and is most sensitive to pp neutrino extraction. The Borexino experiment has extensively studied this. The second issue is distinguishing Cherenkov light from scintillation light to determine the direction of the neutrino and suppress the background. Note that while an event-by-event measurement is not yet feasible, a statistical measurement of the direction of neutrinos has already been explored in PRL 128 091803, 2022. Our proposal for slow LS will be discussed later for a possible event-by-event directionality.

In solar neutrino detection, the dominant background sources are internal radioactivity from the decay of radioactive isotopes within the scintillator and cosmogenic isotopes generated by cosmic muon spallation. These backgrounds pose a significant challenge as they can mimic the signals from neutrino elastic scattering, making it challenging to isolate the true neutrino events. The principal radioisotopes contributing to internal background include ^{40}K , ^{85}Kr , and members of the ^{232}Th , ^{238}U , and ^{210}Pb decay chains. Mitigation of this internal background relies heavily on careful material selection and a multi-stage purification process applied to the liquid scintillator. This process typically involves distillation, liquid-liquid extraction (*e.g.*, water extraction), and gas stripping. Cosmogenic backgrounds are substantially suppressed by the detector's deep underground location, which significantly reduces the cosmic muon flux. Furthermore, residual muons traversing the detector can be efficiently detected and tracked, enabling the removal of most short-lived cosmogenic isotopes through a time veto applied around the muon track. The most persistent cosmogenic isotopes remaining after this veto are ^{10}C and ^{11}C , due to their relatively long half-lives. Further analysis techniques may be employed to discriminate against these longer-lived isotopes; for instance a Three-Fold-Coincidence (TFC) algorithm uses the spatial and time coincidence among those events for enhanced discrimination. The **ν EYE** can achieve radio-purity levels of liquid scintillator comparable as those used in the Borexino experiment. by adopting its purification techniques. Figure 5 shows all known

contributions to background alongside solar neutrinos.

3.4 Reactor neutrino program

There are four nuclear power plants in South Korea and their distances from Yemilab are summarized in Table 3 with their thermal powers. As shown in Table 3, the Hanul reactor complex, the closest to Yemilab, is about 65 km away, which corresponds to the first minimum of the survival probability of $\bar{\nu}_e \rightarrow \bar{\nu}_e$. This positioning suggests that the **ν EYE** detector would be one of the best locations to confirm neutrino oscillations within the three-flavor paradigm.

	Hanul	Wolsong	Gori	Hanbit
Thermal Power (GW)	20.8	11.8	21.3	16.9
Baseline (km)	65	180	216	282

Table 3: List of thermal power and baseline of reactor power plants.

The estimated event rate from the Hanul reactor is approximately 860 events per year. The expected sensitivities are $\Delta m_{21}^2 = (7.51 \pm 0.06) \times 10^{-5}$ eV² and $\sin^2 2\theta_{12} = 0.848 \pm 0.010$ (statistical uncertainties only) for a five-year run of **ν EYE** experiment, as shown in Fig. 7. Since the **ν EYE** detector operates at a similar baseline to that of the JUNO detector, the **ν EYE** experiment is uniquely positioned to validate results for neutrino oscillation parameters from the JUNO experiment over the next decade.

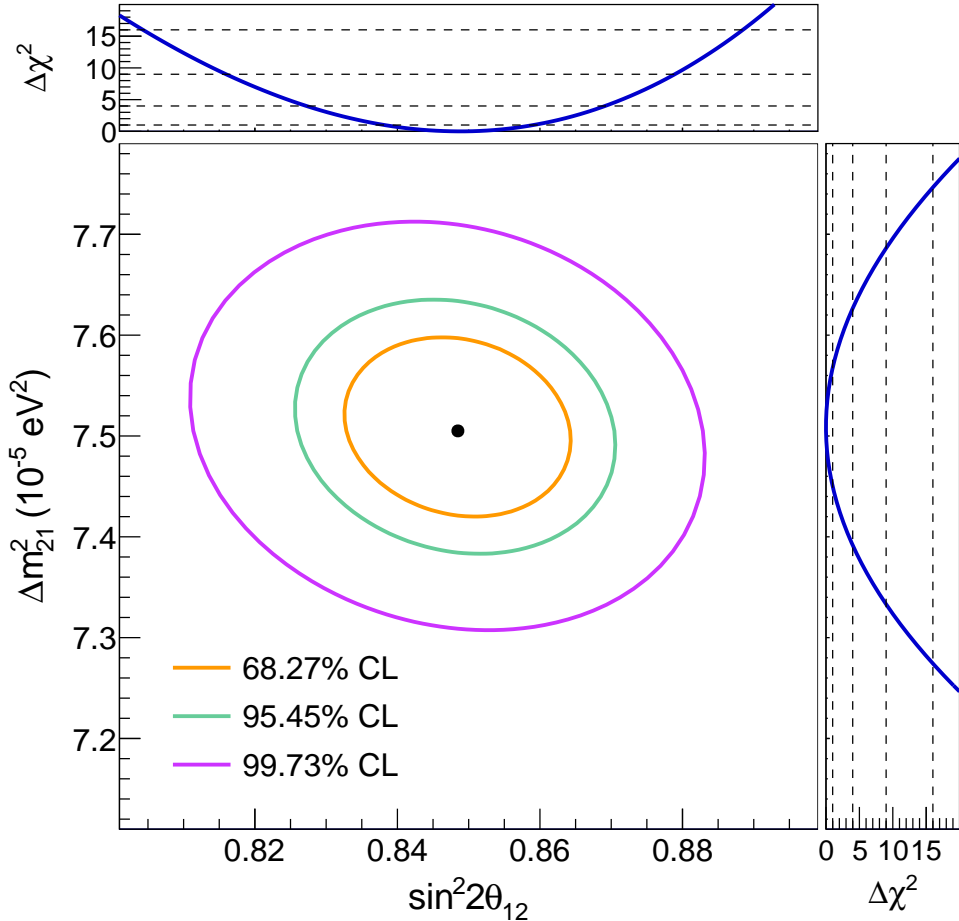


Figure 7: A two-dimensional fit results on Δm_{21}^2 vs. $\sin^2 \theta_{12}$ are shown. Three contours represent different confidence levels. Also projections of $\Delta\chi^2$ differences are shown on top and right.

3.5 Geoneutrinos and astronomical sources

Understanding the inner structure and energy release mechanisms of the Earth is one of the primary interests in geoscience. The localized characteristics of the Earth's crust at various locations can yield valuable insights into plate tectonics and geodynamics.

Geo-neutrino signals originate from natural decays of ^{238}U , ^{232}Th , and ^{40}K , which Borexino (PRD 92 031101(R), 2015) and KamLAND (PRD 88 033001, 2013) have detected from the first two isotopes. The next generation underground neutrino experiments, including **ν EYE**, should conduct further investigations of geo-neutrinos to answer such questions. The most severe background, usually considered as an irreducible background, is $\bar{\nu}_e$ from nuclear reactors. Because

of this, the expected signal-to-noise ratios for the geo-neutrinos vary depending on the locations of underground facilities. The best known site at present is the Chinese [Jinping underground laboratory](#) (CJPL) in China, where one expects an almost background-free environment. On the other hand, the Yemilab site is located approximately 65 km from a nuclear power plant with 21 GW of thermal power. This reduces the signal-to-background ratio to 1/10 initially, as indicated in Fig. 8.

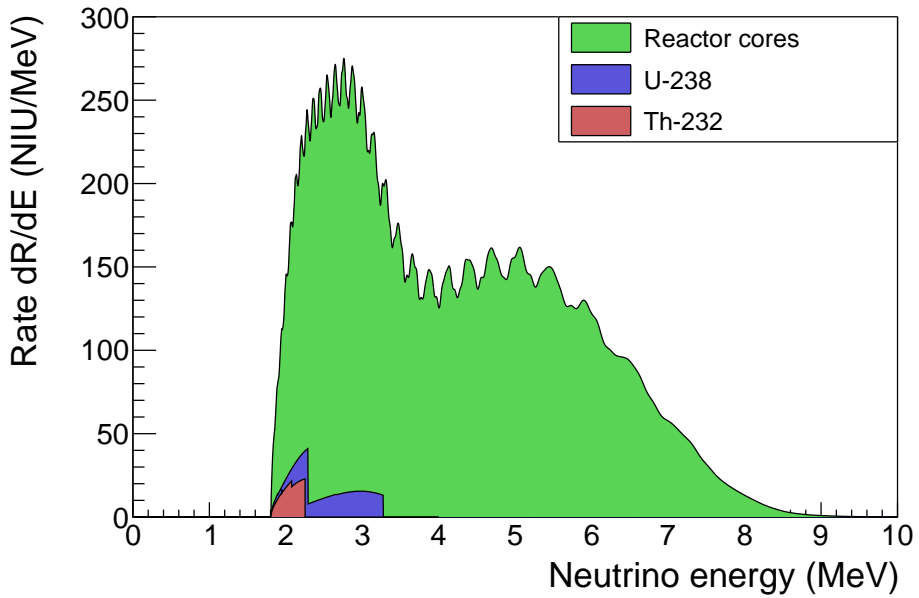


Figure 8: Our estimate of geo and reactor neutrinos with the ν EYE detector.

We intend to implement the requirement for determining the direction of incoming $\bar{\nu}_e$ to significantly reduce the background further and extract the geo-neutrino signal. Furthermore, data collected during periods when the nuclear reactor is not operational—referred to as “off” data—will enhance our understanding of background. We expect to have higher statistics than CJPL but with much larger backgrounds. It is also essential to gather local information about the geo-neutrino near Yemilab site to better understand local plate tectonics.

At the core collapse of a supernova, an estimated of 10^{47} Joules of gravitational binding energy will be released via nuclear weak interactions in form of MeV neutrinos. Such neutrinos have been detected on one occasion by neutrino detectors ([PRL 58 1490, 1987](#), [PRL 58 1494, 1987](#), [PLB 205 209, 1998](#)), albeit with only a few dozen events recorded. Further detection of

supernova neutrinos is of great interest for the supernova physics and for probing novel particle physics properties, which are otherwise inaccessible in laboratories. The expected detection rates for one supernova at a distance of 10 kpc is $\mathcal{O}(100)$ events per kilo-tonne detector (PRD 66, 033001, 2002). We also plot a possible coherent detection of neutrinos (Astroparticle Phys. 36 151, 2012, Astroparticle Phys. 153, 102890, 2023) is shown in Fig. 9 along with the neutrino energy distribution.

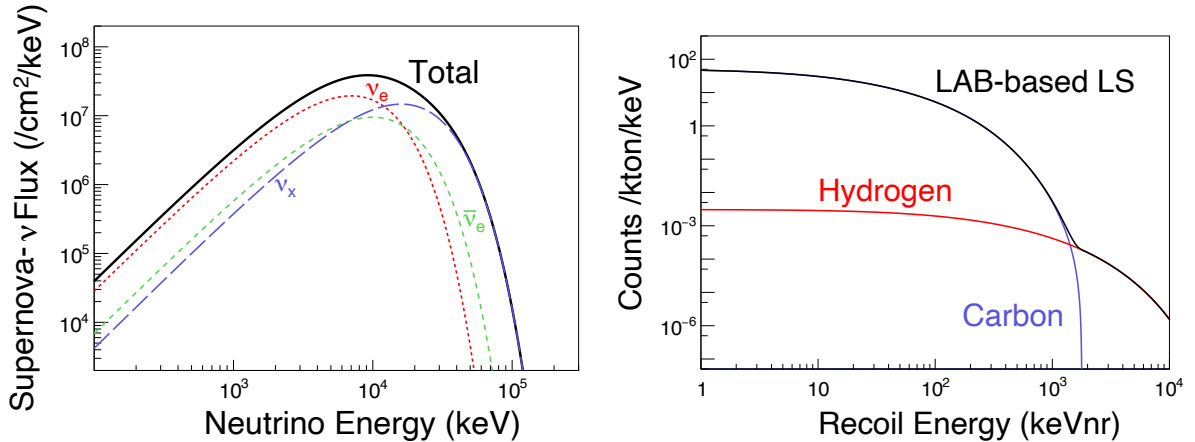


Figure 9: Energy spectra for the supernova neutrinos (left) and the expected nuclear recoil energy spectra of coherent scattering from supernova neutrinos.

Note that the **ν EYE** will be one of the supernova burst detectors in the world (less than 10) and first in South Korea.

3.6 Neutrinoless double beta decay

Experimental sensitivities for the search of neutrinoless double beta ($0\nu\beta\beta$) decay have begun to reach the inverted neutrino mass ordering; however, no evidence for $0\nu\beta\beta$ signal has yet been detected. The current best upper limit on the effective Majorana neutrino mass, $m_{\beta\beta} < [28-122]$ meV at a 90% confidence level (CL), was achieved by KamLAND-Zen (Phys. Rev. Lett. 135, 262501, 2025). It used 745 kg of enriched ^{136}Xe loaded into the LS detector.

The **ν EYE** detector can be turned into a decent $0\nu\beta\beta$ search detector that is competitive with existing and other planned experiments when it is loaded with an appropriate $\beta\beta$ -decay candidate isotope.

One possible candidate isotope is Tin-124 (^{124}Sn) with $Q=2.2$ MeV. It has abundance of 5.79% but shows high solubility in aromatic solvent in the form of organo-tin such as tetramethyltin (TMSn) or tetrabutyltin (TBSn), and the loaded LS demonstrates relatively small light quenching according to a pioneering study ([Astroparticle Phys. 6, 412, 2009](#)).

Another possible choice is ^{130}Te that has a $Q = 2.54$ MeV. It has relatively high natural abundance of 34.1%. We plan to have a long-term R&D for double beta candidates, and loading methods into LS, in order to reach the half-life time sensitivity of order 10^{28} years.

3.7 Detector

In this session, we discuss the **ν EYE** detector design R&D and optimization status. Note that our default detector is widely used LAB based LS. Below we discuss R&D beyond our default LS.

3.7.1 The **ν EYE** detector

- **The detector geometry**

Our proposed structure of the detector consists of

- Target : the central sensitive part of the detector with LS inside an acrylic tank.
- Buffer : the buffer part that removes the background.
- Veto : the veto of cosmic rays and external backgrounds.

The currently considered geometries for the **ν EYE** detector are illustrated in Fig. 10. The left panel shows a spherical frame for the LS, while the right panel presents a cylindrical configuration. In both designs, the buffer consists of a stainless steel tank or structure filled with water or mineral oil, with a diameter of 17 m. For the cylindrical option, the height is 17 m. Surrounding the buffer, a water tank serving as a veto system is positioned, measuring 20 m in height and 19.5 m in diameter.

Our preferred design is base on the spherical geometry, due to its enhanced capability of the background reduction. Key design considerations include the number of PMTs, the volume and

mass of LS inside an acrylic tank, and the effective target volume. Table 4 summarizes the key parameters of the two target configurations.

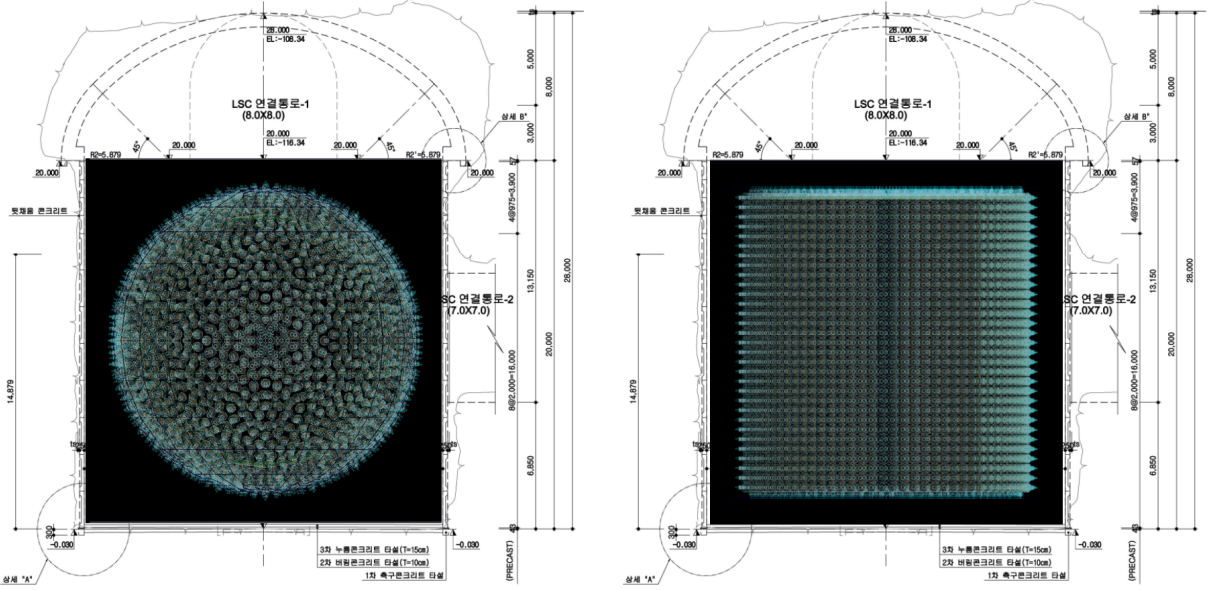


Figure 10: Left: the LS acrylic tank is placed in spherical frame, and right: the LS is contained in a cylindrical frame.

Shape	Cylindrical	Spherical
Radius (m)	7	7.25
Height (m)	14.5	-
Volume (m ³)	2232	1596
Mass (kg)	1920	1373
Number of PMTs	3700	3000

Table 4: A possible target (LS) geometries between cylindrical and spherical shape.

• Reconstruction of IBD

In order to develop the reconstruction algorithm for IBD events, we first place the ^{144}Ce radioactive source at the coordinate (9.5,0,0) m in Geant4 where (0,0,0) m is the center of the **ν EYE** detector. The locations of the IBD events are shown in Fig. 11 where the event vertices are more densely populated near the source.

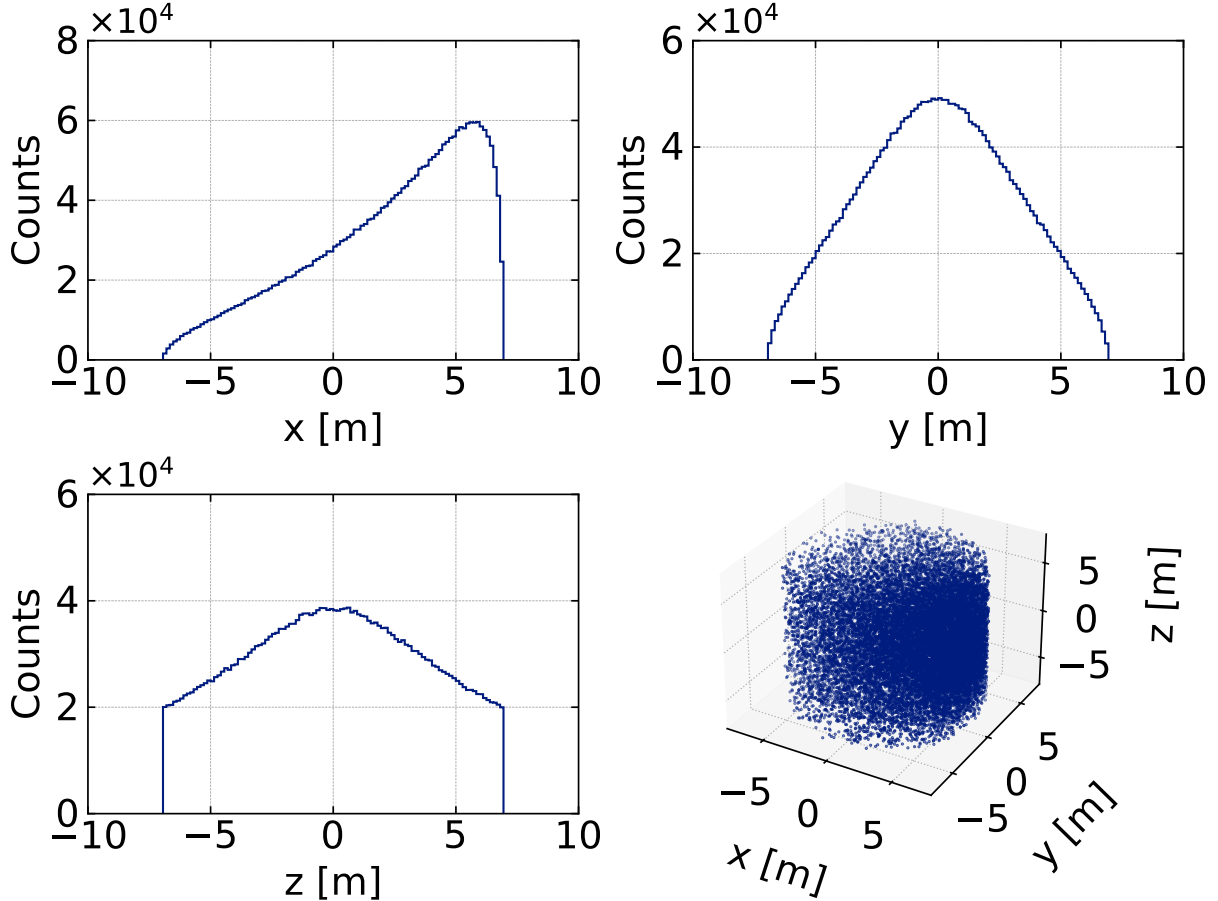


Figure 11: From the left, x , y , and, z position of IBD events are shown. The rightmost scatter plot shows the 3-dimensional plot of vertices.

The detection principle of the IBD is the prompt detection of light from e^+ annihilation, followed by the subsequent detection of light resulting from delayed neutron capture. The timing of the delayed capture is on the order of $\mathcal{O}(200)$ μs , with a 2.22 MeV gamma emission. Based on this detection principle, we implement the following steps to trigger IBD events:

- Require hits in 200 ns.
- If the number of photoelectrons (NPE) exceeds 400, all hits in the 500 ns window constitute the trigger cluster (S1).
- The second cluster is required to have the same condition (S2).

Figure 12 shows the NPE distributions in 250 μs window for one event (on the left). The central

(right) plot has a zoomed view of S1 (S2) NPEs.

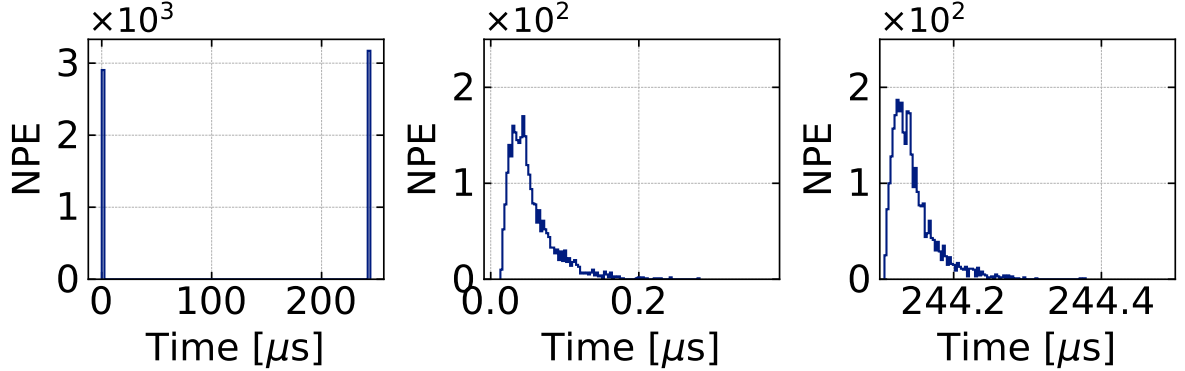


Figure 12: The NPE distributions in $250 \mu\text{s}$ window for one event (on the left). The central (right) plot has a zoomed view of S1 (S2) NPEs.

Once S1 (prompt signal) and S2 (delayed signal) are reconstructed, we analyze the time difference and deposited energy distributions. These are shown in Fig. 13.

- The neutron capture time is found to be $214 \mu\text{s}$ on average.
- The characteristic 2.22 MeV peak for S2 is clearly visible.
- The overall efficiency of IBD reconstruction is approximately 94.6%

This demonstrates the robustness of our detection and reconstruction approach for IBD events.

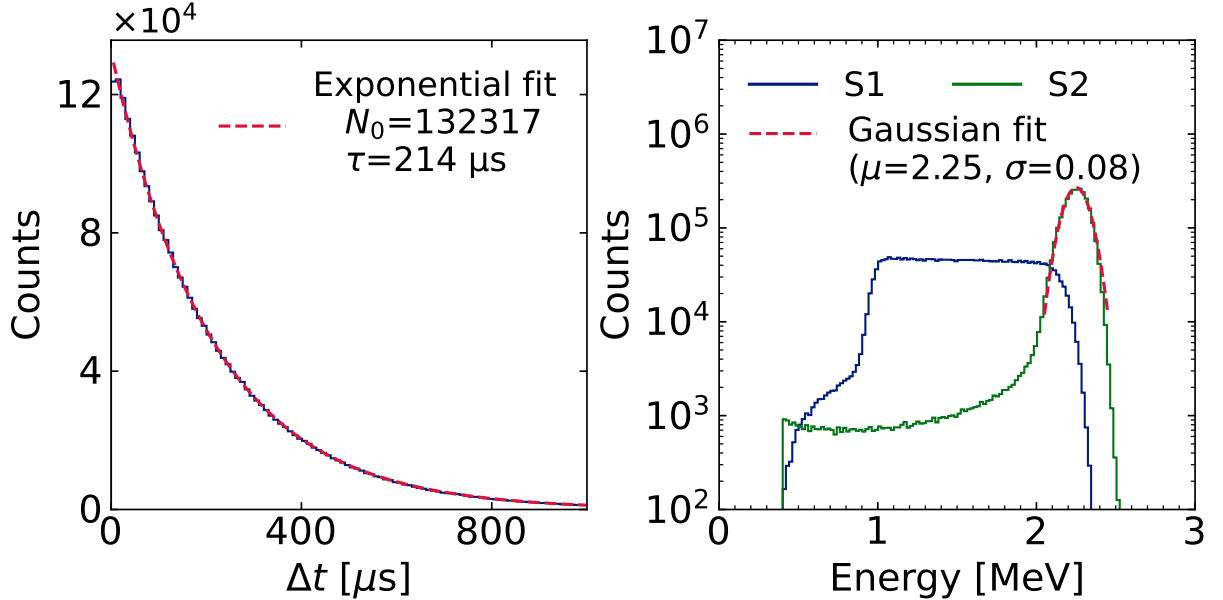


Figure 13: The time difference between S1 and S2 (left) and their deposited energy distributions of them (right) are shown.

3.7.2 One-Tonne Prototype Detector

In order to validate technical issues from the target LS to the data readout chain, one-tonne prototype detector is under construction at the **ν EYE** site. It also allows to measure the intrinsic background to a certain level, perhaps down to 10^{-13} or -14 g/g. The experience we accumulate from operating this prototype will play a key role in the construction and operation of the **ν EYE** telescope. Here we discuss design and the construction status of the prototype detector.

First of all a polyvinyl structure is constructed at the **ν EYE** experimental site. The area is 12 m \times 6 m with the baseline height of 4 m. The top area is extended as an asymmetric triangular type, allowing maximum total height of 5.5 m. A bird's-eye view of this tent structure is shown in Fig. 14. This allows us to have temperature controlled space to operate the one tonne detector as well as to isolate from the outside to a certain extent.



Figure 14: A picture of the housing structure for the one tonne prototype detector is shown. The area is 12 m \times 6 m with the baseline height of 4 m. The top size is extended as an asymmetric triangular type, allowing maximum total height of 5.5 m.

The outer cylindrical stainless steel for the buffer has both diameter and height to be 2.2 m. Inside, we place 1.2 m \times 1.2 m (diameter and height) acrylic tank as the target container,

providing roughly 1 tonne of LS. A Geant4 implementation of the outer stainless steel with the target acrylic tank and PMTs are shown in the left of Fig. 15 and a photograph of the outer container is shown in Fig. 15.

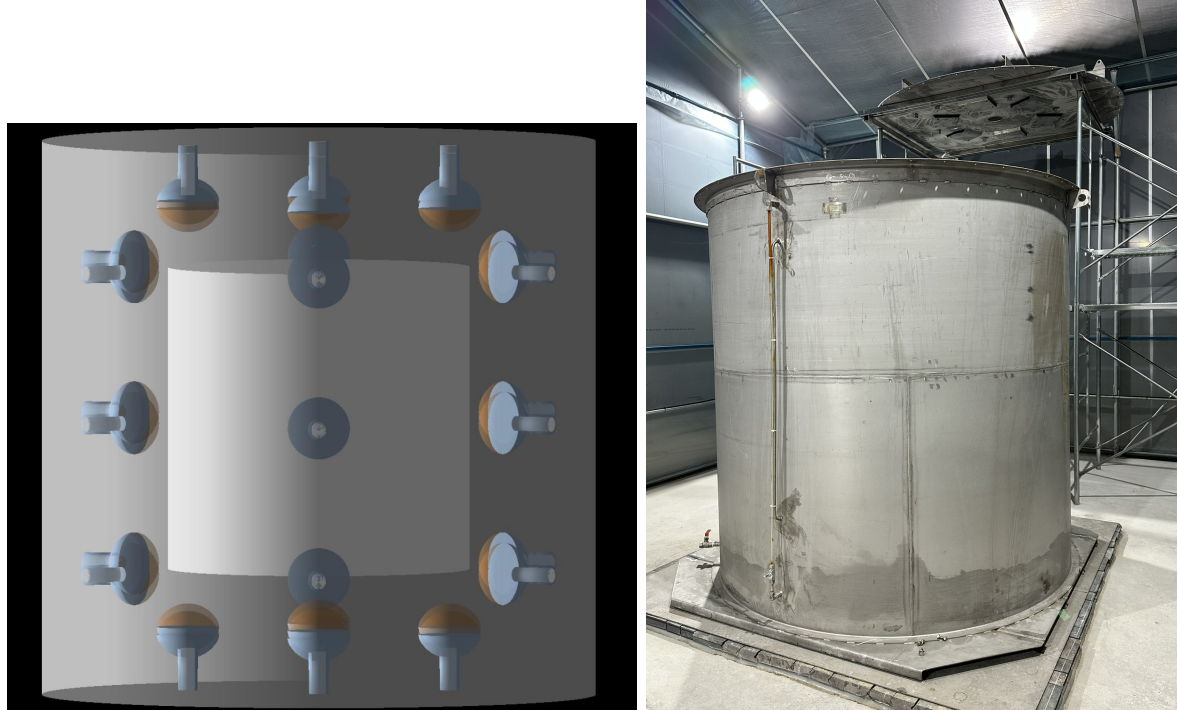


Figure 15: A Geant4 implementation of the outer stainless steel with the target acrylic tank and PMTs is shown in the left. A photograph of the outer container is shown in the right.

In order to place PMTs accurately, we designed a two-dimensional CAD drawing of inner acrylic container, PMTs, and outer tank and is shown in Fig. 16. We expect to mount 31 PMTs in total and the acrylic container under delivery.

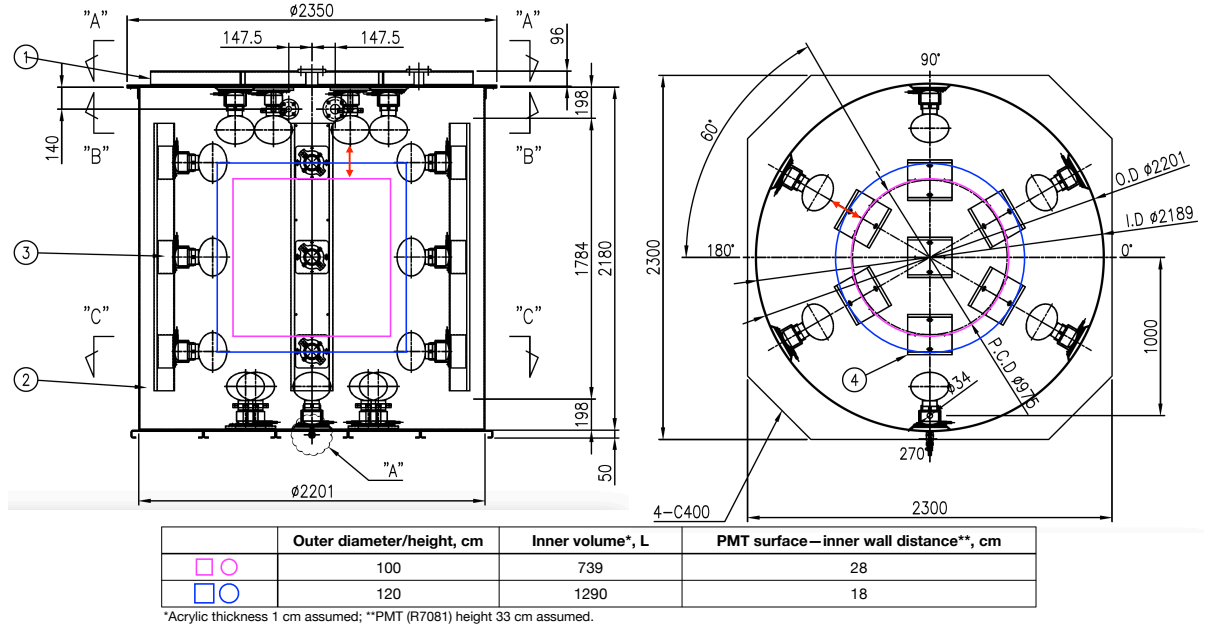


Figure 16: CAD drawings of outer and target containers with PMTs are shown. The left figure is a side-view and the right one is the top view.

We re-use 10 inch PMTs from the RENO experiment (Hamamatsu R7081). To do that, all the PMTs from the RENO detector has been dismounted from the support structure, transported to the Yemilab site, and eventually, cleaned. In total, we collected 67 water-proof PMTs when we need to select 31 PMTs for the prototype detector. We also collected 354 oil-proof PMTs for future usage.

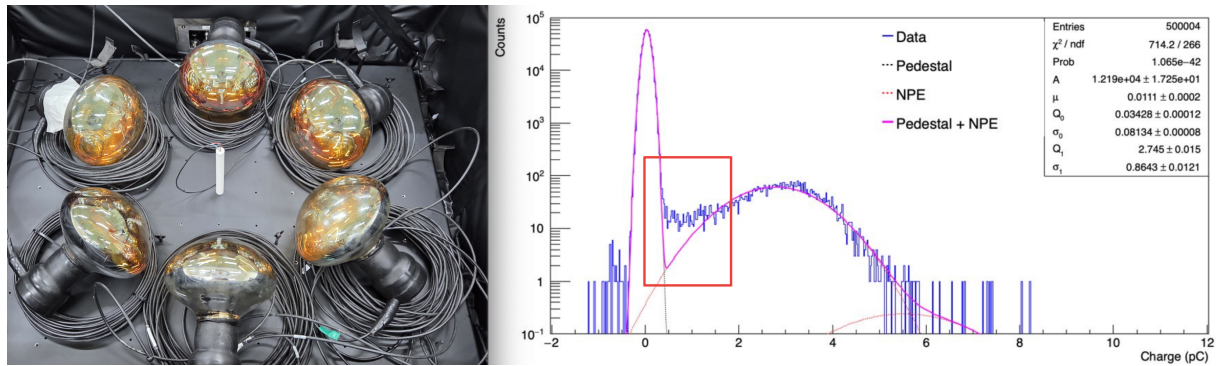


Figure 17: A picture of 6 PMTs in the dark box for the calibration with LED is shown. An example of the single photoelectron signal with the pedestal distribution is shown with the fit in the right histogram.

Then calibration is being carried out to all PMTs with the LED signal, optimized to produce the single photoelectron signal. During this calibration, we check the gain, linearity of the gain, and the dark rate of each PMT. We also take “after pulse” data during the calibration in order to characterize the after-pulse signal later. A picture of 6 PMTs in the dark box for the calibration with LED and an example of the single photoelectron signal with the pedestal distribution is shown with the fit in the right histogram in Fig. 17.

In parallel with the construction of the one tonne prototype detector, a LS purification system for one tonne LS is developed and installed in the housing. Figure 18 shows a picture of such purification system installed. It includes filtration at this moment. The water extraction and Nitrogen gas stripping will be added later.



Figure 18: A picture of our LS purification system installed in the housing is shown. It includes filtration at this moment and in future, water extraction and Nitrogen gas stripping will be added.

Note that even with one-tonne detector, one can address production mechanism of TeV-scale muons in extensive air shower underground, where so called “muon puzzle” is under discussion [arXiv:2510.16341](https://arxiv.org/abs/2510.16341).

3.7.3 Slow LS

In the order of $\mathcal{O}(\text{MeV})$ and sub-MeV neutrino detection, a large part of the background arises from radioactive decays in the detector itself. Therefore, tremendous efforts have been made to have a radio purification system near the detector. The decay of radioactive material is random in direction but the neutrinos of interest are directional, such as neutrinos from a radioactive source or from the Sun.

The scattered electrons in the LS generate both scintillation and Cherenkov lights, and neutrino’s direction can be reconstructed if the Cherenkov light is detected. However, the amount of Cherenkov light is far less than that of scintillation and usually undetected. The separation of Cherenkov and scintillation significantly improves background rejection and signal efficiency.

This hybrid detection can be achieved by following methods:

- Development of LS with slow scintillation time to separate Cherenkov light.
- Fast photon detectors.
- Spectral sorting.

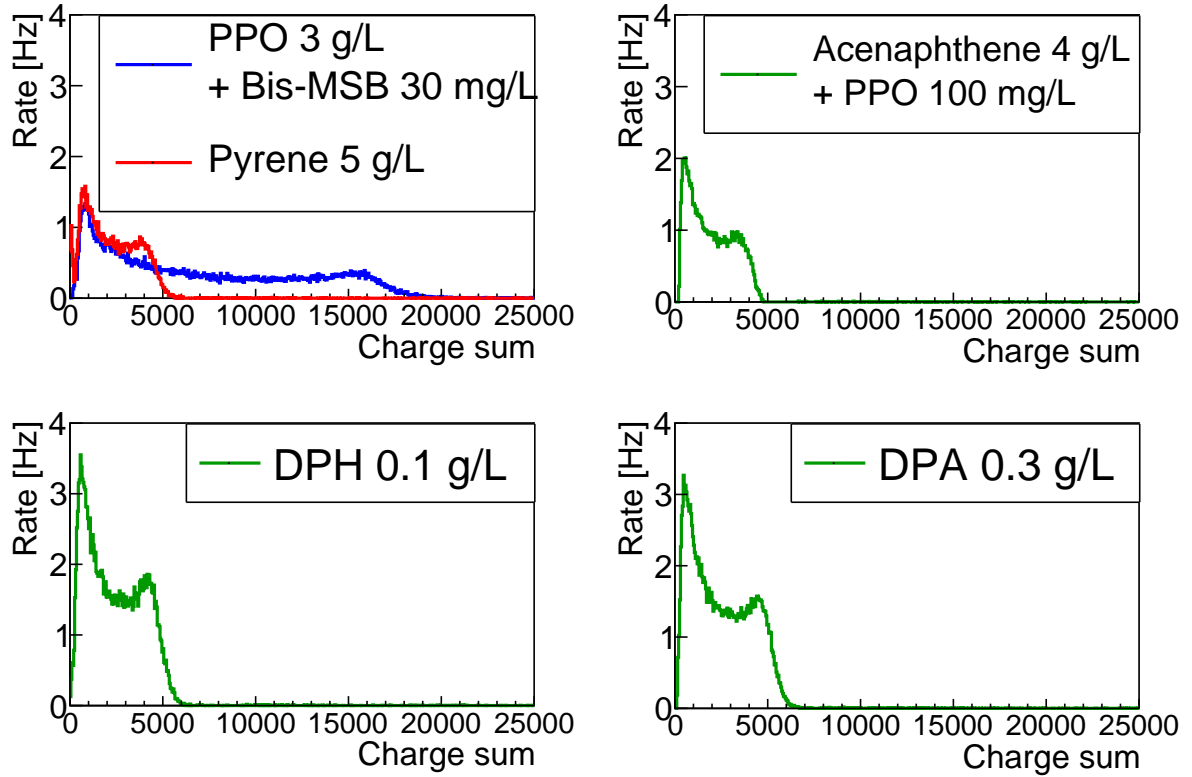


Figure 19: Relative light yields for PPO+Bis-MSB, pyrene, acenaphthene + PPO, DPH, and DPA are shown. The combination of PPO+Bis-MSB shows the highest light yield.

Our primary target R&D is the first item, the slow LS. We will briefly mention our R&D for the fast photon detectors. The spectral sorting ([Phys. Rev. D 101 072002, 2020](#)) in principle works but becomes very expensive for the **ν EYE** experiment. We also find the fast photon detector has a similar issue.

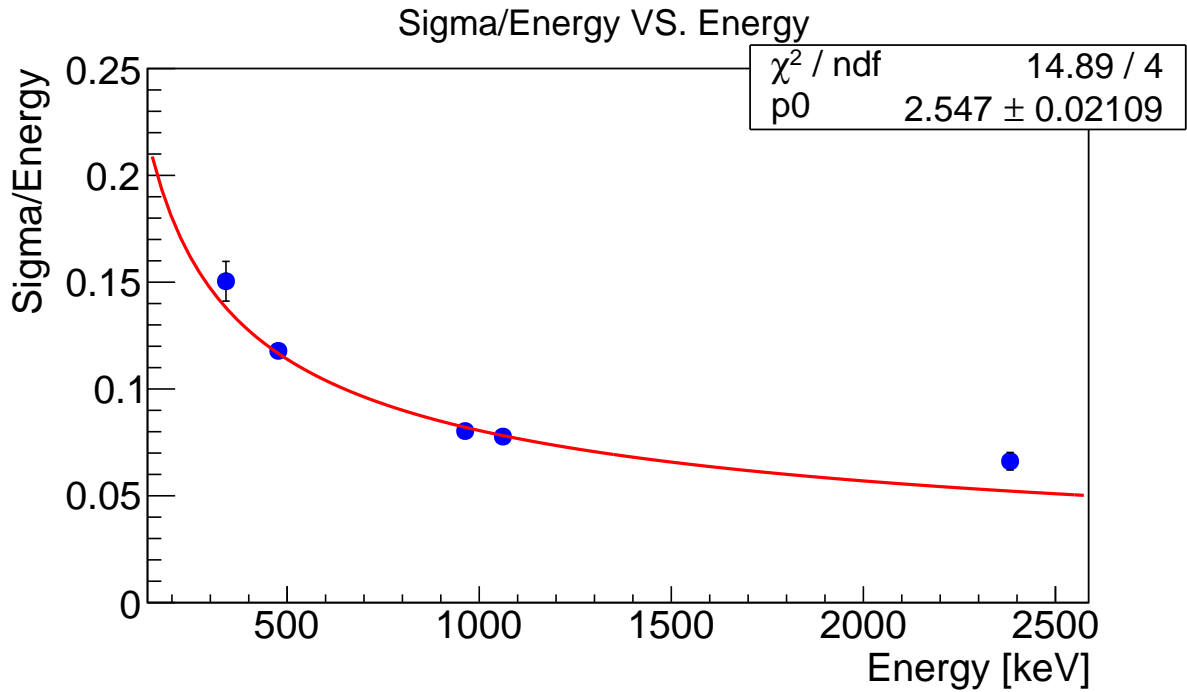


Figure 20: The relative energy resolution as a function of the source energy is shown. Points are measurements with various radioactive sources and the curve is the fit to points.

For a slow LS R&D, we start with mixtures of linear alkylbenzene (LAB) and fluors, motivated by [NIMA 972 164106, 2020](#). For fluors, we use PPO 3mg/L + Bis-MSB 30 mg/L, pyrene 5 g/L, acenaphthene 4 g/L + PPO 100 mg/L, DPH 0.1 g/L or DPA 0.3 g/L, to measure relative light yields, energy resolution, absorbance*, and emission spectra. A small acrylic vessel with a diameter of 60 mm and a height of 50 mm is prepared as a container for LS. Relative light yields for PPO+Bis-MSB, pyrene, acenaphthene + PPO, DPH, and DPA are shown in Fig. 19. The combination of PPO+Bis-MSB shows the highest light yield.

*The logarithmic ratio of incoming and transmitted radiant power.

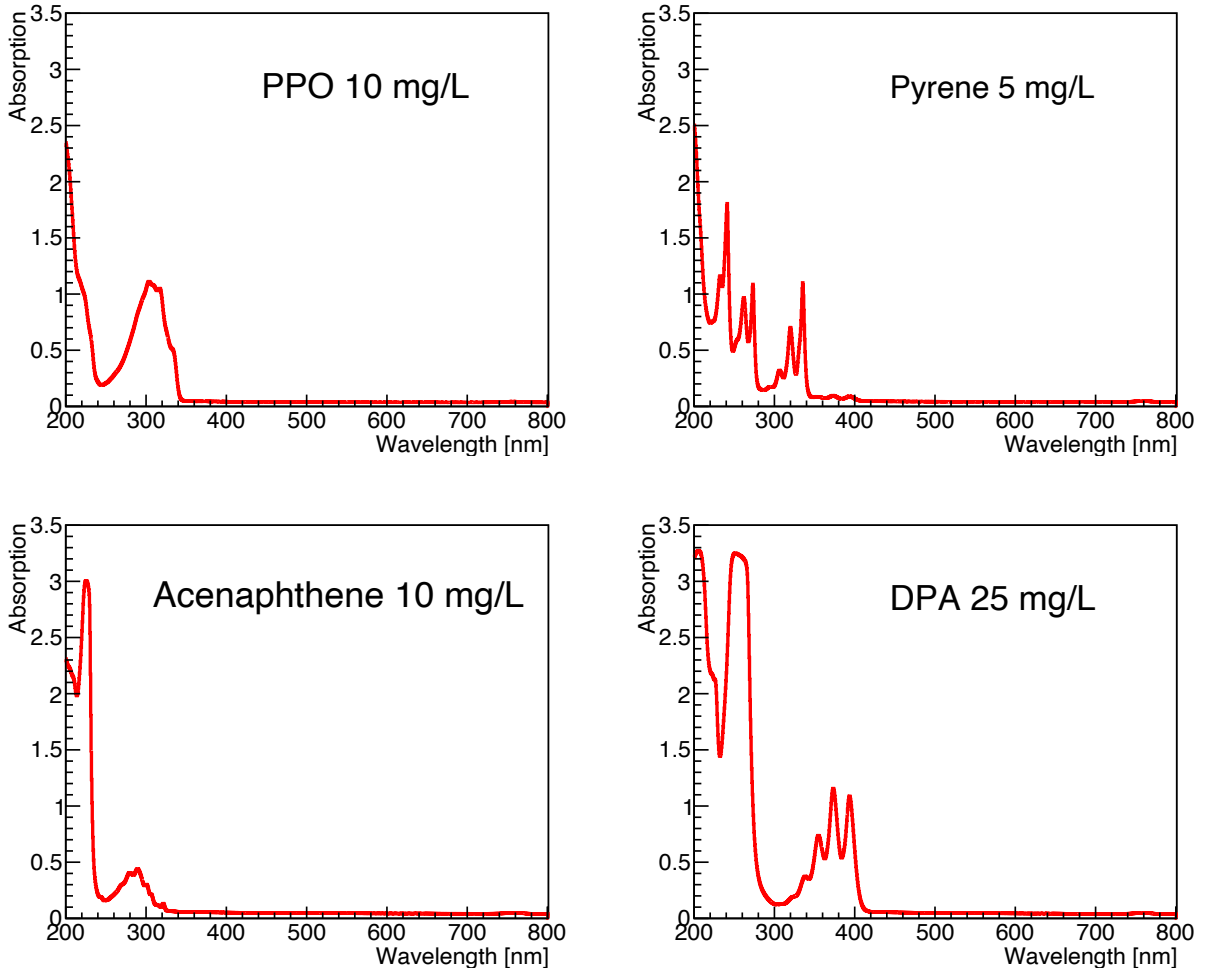


Figure 21: Absorbances for PPO+Bis-MSB, pyrene, acenaphthene + PPO, and DPA as a function of the wavelength are shown.

The energy resolution is measured with radioactive sources and the Geant4 simulation, and the result is shown in Fig. 20. The fit to the data points yields $\sigma/E = 2.55 \pm 0.02 (\sqrt{\text{keV}})/\sqrt{E} (\text{keV})$. Note that the container is relatively small, so the resolution is about 8% at 1 MeV.

The absorbances for all five LS targets are also measured and shown in Fig. 21. Note that both the relative light yields and absorbances agree with previous findings ([NIMA 972 164106, 2020](#)). We also developed a Geant4 simulation setup of a prototype detector, for the simulation study of LS. The pyrene LS detector is contained in an acrylic structure with a diameter of 1.2 m, a height of 1.2 m and a thickness of 1 cm. This corresponds to 1.2 tonnes of LS. There is a buffer made of stainless steel with a diameter of 2.2 m and a height of 2.2 m. The buffer is currently

filled with water. There are 140 PMTs of 10 inches placed, motivated by [Hamamatsu R7081 PMT](#). Note that the quantum efficiency is 25% at the wavelength of 390 nm. Fig. 22 (left) shows the geometry of the prototype LS detector. The PMT hit time distribution is obtained from this geometry, shown in Fig. 22 (right). The emission and re-emission spectra are also checked. We plan to construct this prototype detector in the early stages of the project to learn as many technical details as possible about the slow LS properties.

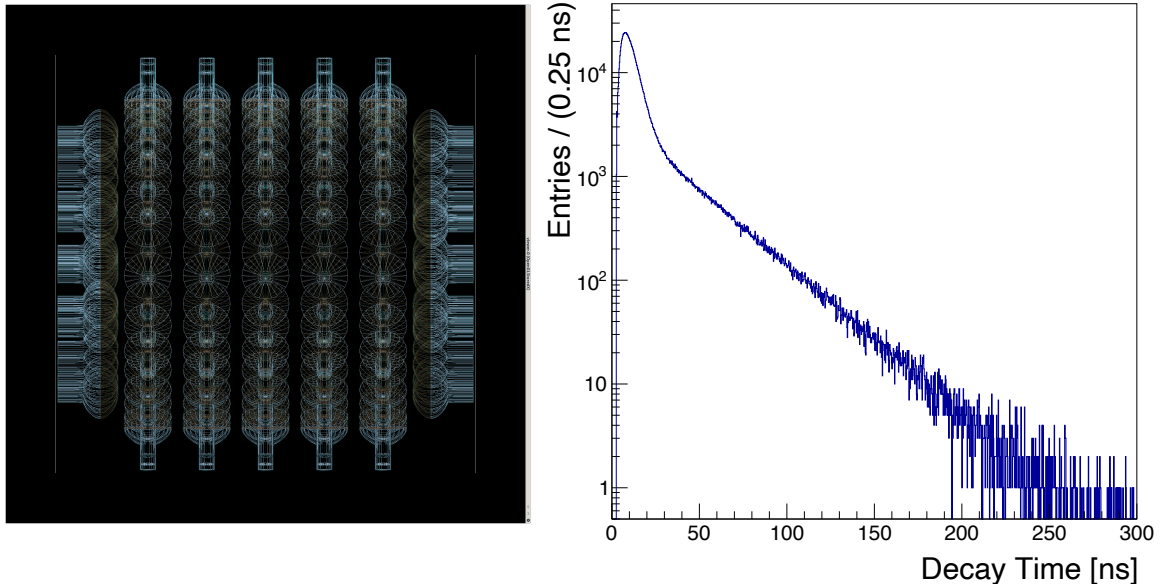


Figure 22: A prototype LS detector geometry is on the left. The LS scintillation time seen by PMTs is on the right.

We also studied the Cherenkov light separation capability in the Geant4 simulation. This was done with the two-kilo-tonne **ν EYE** detector geometry setup which will be described in detail later. We introduce the PMT hit timing correction with the formula

$$t = t_{\text{meas}} - \frac{|\mathbf{r}_{\text{rec}} - \mathbf{r}_{\text{PMT}}|}{c/n}, \quad (3.1)$$

where t_{meas} is the measured time. The \mathbf{r}_{rec} and \mathbf{r}_{PMT} are reconstructed vertex and each PMT

location 3-vectors. Here, c and n are the speed of light in vacuum and the index of refraction of the LS. Our Geant4 simulation of hit-time distributions with the **ν EYE** detector setup, with (red) and without (blue) timing correction are shown in Fig. 23. From the left, the pyrene concentrations are, 8, 4, and, 2 g/L, respectively. Note that the separation depends on the concentration of pyrene in LS. Here we assume 10 cm vertex reconstruction resolution and the transient time spread of 1 ns.

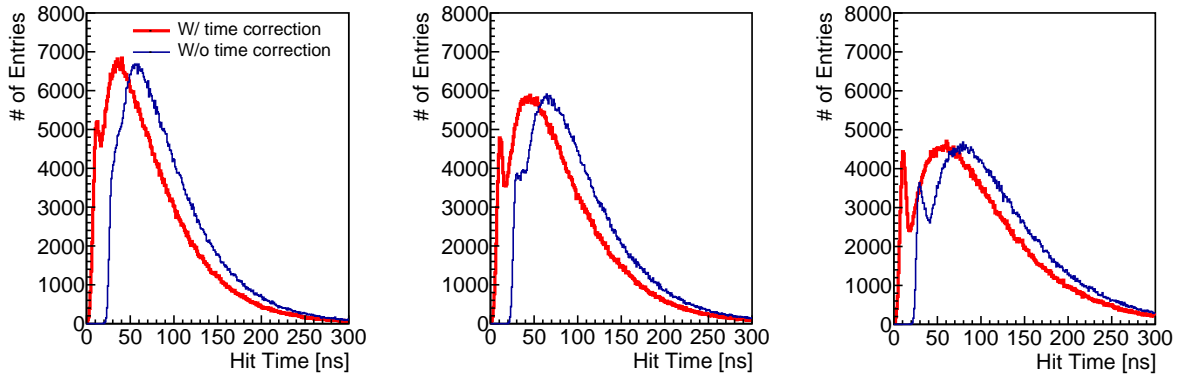


Figure 23: Our Geant4 simulation of hit-time distributions with the **ν EYE** detector setup, with (red) and without (blue) timing correction described in the text. From the left, the pyrene concentrations are, 8, 4, and, 2 g/L, respectively.

We would like to emphasize that the increase in the separation capability of Cherenkov light in the slow LS is obtained at the cost of the light yield in general. Our main R&D is to see if there is an optimum balance between the two competing issues.

3.7.4 Photodetector

The photodetector is the most significant portion of the budget in large-size neutrino telescope such as **ν EYE**. Here we briefly mention two technologies.

• PMT

In Table 5, we list several candidate photodetectors and discuss their properties. Hamamatsu PMTs have been well studied already by Yemilab team and therefore not mentioned here. We plan to study further 8 inch PMTs by NVT in near future since they offer competitive performance with reduced production cost. This one will be used in [Jinping Neutrino Experiment](#).

Model	R12860	N6203	N6082
Size (inch)	20	20	8
Peak wavelength (nm)	420	380	380
HV (V)	2000	1900	1750
Q.E. (%)	30	30	30
TTS (ns)	2.4	5	1.6
Supplier	Hamamatsu	NVT	NVT

Table 5: Comparison between selected PMTs available at present. Hamamatsu is a Japanese and NVT is a Chinese company.

• LAPPD

The LAPPD (Large area picosecond photodetector, [NIMA 958 162834, 2020](#)) is a planar geometry photodetector based on the micro channel plate (MCP) technology. The basic properties are summarized in Table 6.

Area (mm ²)	200 × 200	HV	−2100 V
Gain	10^7	Q.E.	> 30%
Timing	55 ps	MCP	2 layers

Table 6: A list of parameters for the LAPPD.

To understand the operational characteristics of LAPPD, we rented a second-generation, capacitor-coupled 64-pad LAPPD from [Incom, Inc](#) in the US. For triggers, a cubical bulk plastic scintillator is placed with top, bottom, and side (right surface) PMTs. The LAPPD is attached to the left surface of the scintillator as shown in Fig. 24 left. In total 48 signals are read out by CAEN 5742 digitizers. A cosmic muon signal is shown in Fig. 24 right. A couple of channels may have low gains.

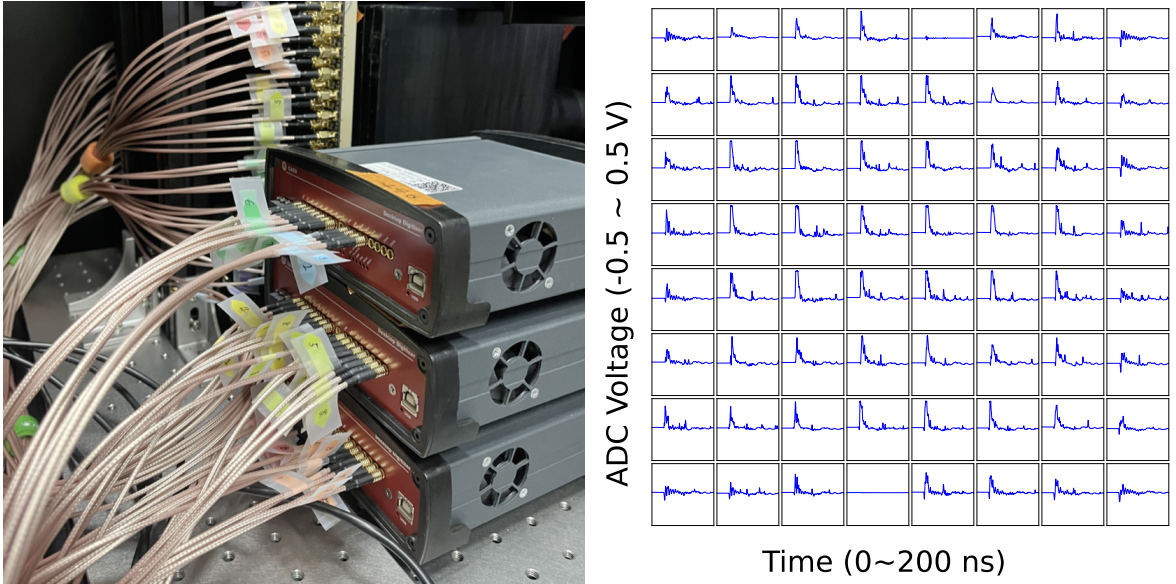


Figure 24: A cosmic muon-induced scintillation light detection setup (left). The right picture shows signals from 48 channels.

We also prepared a motor-controlled $x - y$ stage with a mounted LED for gain correction. The LAPPD is positioned face-up, while the $x - y$ stage moves the downward facing LED to illuminate specific pixels. The setup (left) and the calibrated (set to 0) LED signals are shown in Fig. 25.

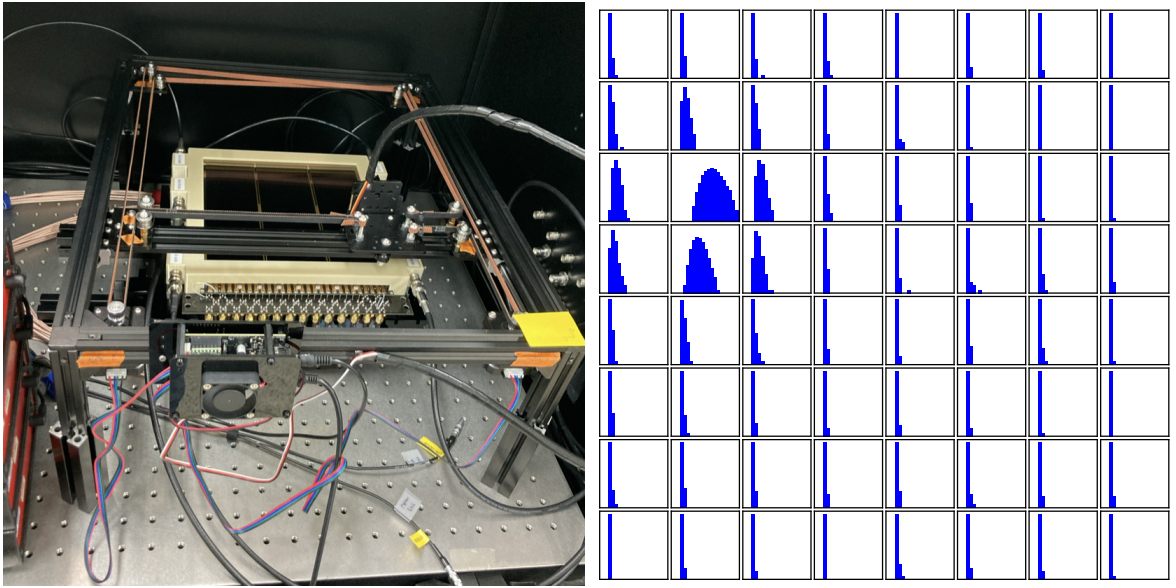


Figure 25: A picture of automatic $x - y$ stage (left) and the gain calibration result with LED (right). The location of the LED is on the channel with the largest signal (C2).

After four-month rental period, we tentatively concluded that LAPPD is an attractive option for the **ν EYE** experiment, assuming its internal background is at least as low as the case of the PMT. However, for LAPPD to be our primary choice of the photodetector, a significant reduction in cost is necessary at this stage. Additionally, a suitable “base” or voltage divider must be provided to supply different voltages to the photocathode, two MCPs (top and bottom), and the electric ground.

3.7.5 Environmental Backgrounds

In the Yemilab **ν EYE** experimental hall, samples of shotcrete and rock are collected for analysis⁴, and the activities of ^{238}U , ^{40}K , and ^{232}Th , are measured. The results of these measurements are summarized in Table 7, where all units are in Bq/kg.

	^{238}U	^{40}K	^{232}Th
Shotcrete	16.7 ± 0.6	447 ± 16	25.3 ± 0.6
Rock # 1	19 ± 2	618 ± 69	22 ± 2
Rock # 2	18 ± 2	872 ± 98	26 ± 2
Rock # 3	13 ± 1	561 ± 63	15 ± 1

Table 7: Measured radio activities of ^{238}U , ^{40}K , and ^{232}Th in shotcrete and three rock samples. All numbers are in units of Bq/kg.

We also measured the background energy spectra at various locations in the hall, including the floor, mid-tunnel, and top-tunnel areas. The results, categorized into six different energy bands, are presented in Fig. 26. While different colors represent measurements taken at different locations, no significant variations in the spectra were observed across these areas.

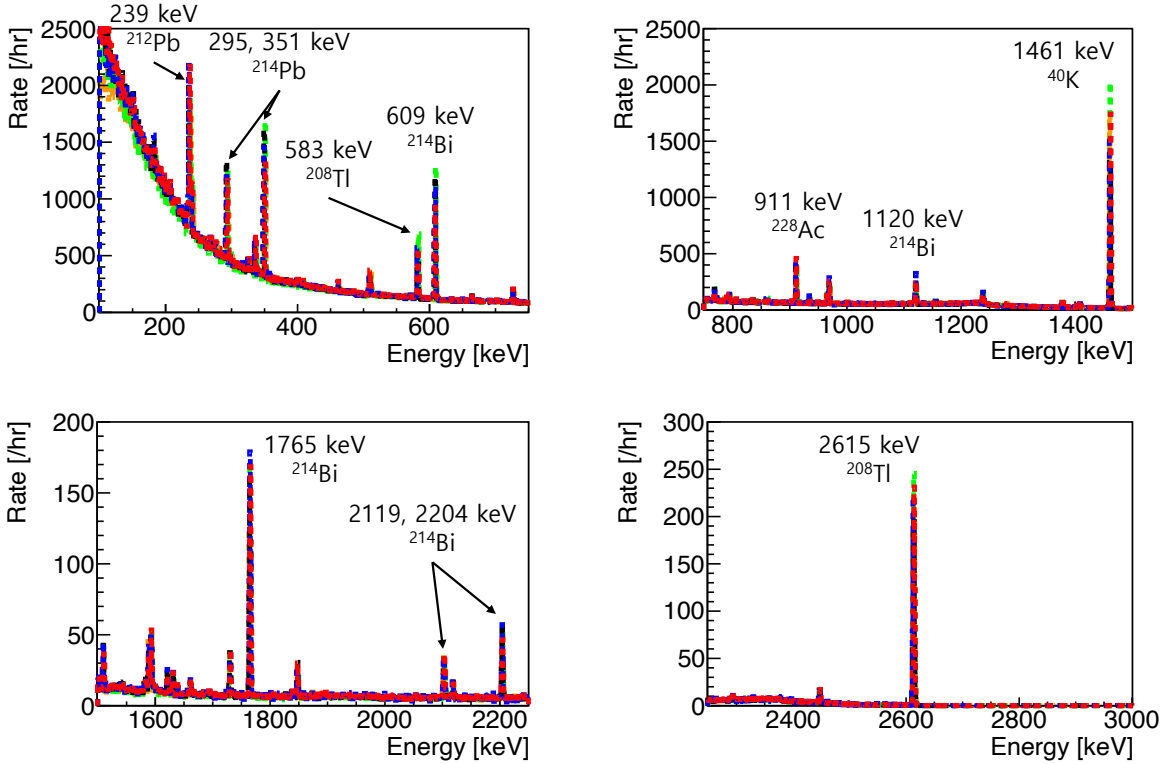


Figure 26: The HPGe measurements are shown. Histograms correspond to, from the top left to bottom right, [100, 750] keV, [750, 1500] keV, [1.5, 2.3] MeV, [1.5, 2] MeV, and [2.3, 3.0] MeV ranges.

We also measured the Radon activity in the hall and results are summarized in Table 8.

Location	Radon level (Bq/m ³)
Up	68 \pm 14
Middle	84 \pm 19
Middle (opposite)	118 \pm 12
Middle (low)	125 \pm 21
Hall center	148 \pm 17

Table 8: Measured Radon activity in several locations in the ν EYE hall.

This measured environmental activity is being implemented in our full Geant4 detector setup. Note that we plan to install dedicated Radon reduction systems in the experimental site to suppress the Radon level sufficiently.

3.8 R&D on next generation neutrino detector

The LS is our primary choice for the detector since it is a well developed and understood technology, over the last 60 years. However, despite its advantage, the LS technology does not allow the separation of Cherenkov from scintillation lights easily and the particle identification is also difficult. Due to Cherenkov radiation occurs at a faster rate than scintillation; it is emitted instantaneously, whereas scintillation light results from several molecular de-excitation processes that exhibit a slower decay time constant with characteristic features, new kinds of technologies have been discussed in the neutrino community. Here we discuss our next generation neutrino detector R&D and approach.

3.8.1 Water based LS

Water-based Liquid Scintillator (WbLS) is a hybrid detection medium formulated by dispersing LS into pure water using surfactants. It has been proposed to combine the advantages of both water Cherenkov and LS detectors. This novel medium is currently being implemented and demonstrated in several experimental efforts: [Phys. Rev. C 95, 055801 \(2017\)](#), [Phys. Rev. C 95, 055801 \(2017\)](#), [Eur. Phys. J. C 80, 416 \(2020\)](#), and [JINST 18, P02009 \(2023\)](#).

Structurally, the organic scintillator molecules are encapsulated within micelles, which are suspended in the aqueous medium. This technique aims to take the advantages of both LS and water: the high light yield and low energy threshold of LS, and the high transparency, low cost, and directional capabilities of water Cherenkov detectors. WbLS is predominantly water, which allows us to optimize the scintillation light yield by adjusting its concentration depending on the physics goals of the experiment.

The primary motivation for developing WbLS is to achieve “hybrid detection” with the discrimination of Cherenkov and scintillation signals. In a conventional LS detector, the isotropic and intense scintillation light typically overwhelms the Cherenkov light. However, in WbLS, the two lights can be separated due to the reduced scintillation light yield and the distinct features of the two lights. Cherenkov radiation occurs at a faster rate than scintillation; it is emitted instantaneously, whereas scintillation light results from several molecular de-excitation processes that exhibit a slower decay time constant with characteristic features. Utilizing these distinct

time profiles, the prompt Cherenkov photons can be distinguished from the delayed scintillation photons. In addition, the characteristic shape of Cherenkov cone and an isotropic shape of scintillation, and photon wavelength profile also can be used to separate the Cherenkov and scintillation signals. This discrimination capability enhances the signal-to-background ratio. It allows us to reconstruct the direction of incident particle with better energy resolution than pure water Cherenkov detectors due to the additional scintillation photons.

While traditional organic LS requires complex chemical formulations to dissolve metallic isotopes, the water phase of WbLS allows for the direct dissolution of hydrophilic metallic salts. This feature is particularly important for loading neutron-capturing agents such as Gadolinium (Gd), which significantly enhances the neutron capture cross-section. The neutron-capture signal provides a robust delayed coincidence tag for identifying Inverse Beta Decay (IBD). From an engineering and safety perspective, WbLS offers distinct advantages over pure LS. Since WbLS typically comprises of 90% water, it is non-flammable and environmentally safer than oil-based scintillators. Additionally, the cost of water is negligible compared to organic solvents, rendering WbLS a cost-effective solution for massive detectors. Furthermore, WbLS offers additional advantages in terms of maintaining the medium by circulation and purification. The aqueous and organic components of WbLS can be separated using nanofiltration system, enabling the removal of the radioactive impurities and purify each phase independently before re-mixing, ensuring long-term stability.

3.8.2 Opaque LS

A new detection technique for neutrinos with an opaque scintillator is proposed recently ([Nature, Commun. Phys. 4, 273 2021](#)). This technique, known as LiquidO in the neutrino community, can provide efficient identification of particles in event-by-event basis through a high-resolution imaging based on optical fibers. A 10 litter scale prototype was fabricated and characterized in detail ([arxiv:2503.02541](#)).

In order to explore this new technology and study a possibility to use it to a 2 kilo tonne scale neutrino detector, we started R&D on the LiquidO technology. The R&D efforts encompass the fabrication of a small-scale prototype as well as considerations for scaling up to larger detector

systems.

3.8.3 Others

We also look at the original idea from Raghavan’s ^{115}In loading with a segmented detector [arXiv:0705.2769](https://arxiv.org/abs/0705.2769). The main idea is to look at the triple-coincidence signals from $\nu_e + ^{115}\text{In} \rightarrow ^{115}\text{Sn}^* + e^-$ and the delayed ($4.76 \mu\text{s}$) reaction of $^{115}\text{Sn}^* \rightarrow ^{115}\text{Sn} + 2\gamma$. In order to realize the delayed triple-coincidence of two γ s and e^- , the detector must be segmented or to be “liquidO” like, in order to reconstruct the event topology. The segmentation with total internal refraction has been explored [arXiv:2507.07397](https://arxiv.org/abs/2507.07397) and [arXiv:1501.06935](https://arxiv.org/abs/1501.06935). The main issue in this case is the huge β decay of ^{115}In background, and the finer segmentation has stronger background rejection in general. We start to look at this approach to see if this approach with the ^{115}In loading is feasible or not, for the pp solar neutrino detection in particular.

There has been attempt to load ^7Li to water based LS since it allows the charged current interaction with about 60 times larger cross section than that from neutrino-electron elastic scattering, as in [Eur. Phys. J. C \(2023\) 83:799](https://doi.org/10.1140/epjc/s10050-023-12089-0). It is relatively easy to make LiCl water solution but it is uncertain how one loads ^7Li in pure LS. Our chemistry team starts to look at possibility to load ^7Li to LS to increase the solar neutrino sensitivity.

3.9 International collaboration

The Korean neutrino community has accumulated 20 years of technological expertise from on-shore and offshore neutrino experiments, positioning the **ν EYE** experiment for success. We may miss the state-of-the-art radio purification experience and the logistics on the high-dose radioactive source.

To address these, we have established a robust international collaboration with Borexino experts through the [IBS-INFN](https://ibsinfn.org) framework of 2024.

The **ν EYE** project has been in regular discussions with the the US IsoDAR team every two months. Additionally, we have ongoing discussions with China for JUNO and the Jinping lab. Japanese neutrino community has always maintained a close partnership with Korean neutrino researchers, especially with the recently launched Korea Neutrino Observatory project. In sum-

mary, a significant part of the global neutrino physics community is already engaged with us, and this collaboration is expected to expand rapidly upon receiving official approval for the project.

4 Construction and Utilization Plan

The construction timeline for the **ν EYE** detector is estimated to be six years, followed by an additional two years dedicated to commissioning. This is consistent with the typical timeline for constructing a $\mathcal{O}(1)$ kilo-tonne neutrino experiment. A major advantage is that the **ν EYE** pit, the purification system area, and the space for the potential IsoDAR accelerator are already prepared, significantly reducing both time and budget during the construction phase.

To ensure the success for the project, we are currently designing a prototype $\mathcal{O}(1)$ -tonne detector. This will help us:

- Validate the LS detector performance,
- Understand radioactive background levels, and
- Refine the construction details for the full **ν EYE** detector.

Additionally, we maintain close collaboration with the Yemilab operation center to finalize the detector construction and installation procedure, including the purification and LS detector system infrastructure.

5 Plan to Organize Research Groups

The **ν EYE** center will be structured with two key committees:

- **Executive Committee:** Responsible for reviewing regular progress, overseeing the hiring process, and managing budget allocation, and spending.
- **International External Review Committee:** Tasked with evaluating annual progress and providing strategic guidance for center's overall direction.

Within the center, there will also be two major research groups, which will focus on different aspects of the **ν EYE** experiment.

- **Instrumentation Group:** Responsible for the detector design, electronics, infrastructure construction, and radioactive source preparation.
- **Physics Group:** Focuses on simulation tool development, detector optimization, and physics analyses.

These groups will work in close collaboration to ensure the success of the **ν EYE** experiment.

In the early phase of the experiment, the hardware group will take on a primary role, focusing on detector construction, electronics, and infrastructure setup. Once the detector is operational, the hardware group will shift its focus to maintenance, while the physics group will take the lead in data analysis, simulation improvements, and physics studies. Both groups expect to work closely to exchange inputs and outputs to develop the experiment most effectively.

The Korean neutrino research community has its roots in the RENO project, which played a crucial role in training and developing a strong pool of neutrino experts over the past 20 years. This proposal brings together experienced researchers who have contributed significantly to past and ongoing neutrino experiments, ensuring that the **ν EYE** project benefits from a highly skilled and knowledgeable team.

The installation of the **ν EYE** experiment will mark the completion of the full scientific program at Yemilab, complementing the experiments of Center for Underground Physics of IBS which doesn't detect neutrinos directly. With the **ν EYE** experiment, Yemilab will establish itself as one of the world's leading multipurpose underground laboratories, contributing to cutting-edge research in neutrino physics and rare event searches.

6 Expected Research Outcome

If the radioactive source experiment yields a positive signal, it would provide strong evidence for the existence of a sterile neutrino, aligning with the results from the BEST experiment. Such a discovery would be profound implications for our understanding of neutrino physics, shedding light on the origin of neutrino mass and opening a new frontier in sterile neutrino research.

Additionally, we aim to study CNO neutrinos from the Sun to address the ongoing tension in metallicity measurements. Precision measurements of ${}^7\text{Be}$, *pep*, and ${}^8\text{B}$ solar neutrinos will allow us to probe the vacuum-MSW transition region of the electron survival probability. This will serve as a critical test of the current neutrino oscillation framework, potentially confirming or challenging our existing theoretical models. In addition to the studies on sterile and solar neutrinos, it will serve the unique supernova burst alert detector in Korea. With the IsoDAR, it will be a unique facility in the world to search for dark sector and non-standard neutrino interactions coupling ultra-low background and high-power accelerator.

The **νEYE** experiment would be an unique reactor neutrino experiment to be able to validate results at 65 km baseline.

7 Implementation Plan by Phase and a Cost Estimate

7.1 Implementation plan

The present implementation plan to operate the **νEYE** detector is described below.

- **Water Cherenkov** Phase (first 6 years)

Our immediate focus is on constructing the detector while finalizing the LS R&D to ensure optimal physics output. Once the detector is built, we will proceed with filling the veto tank with water.

By leveraging Cherenkov light detection, we aim to observe ${}^8\text{B}$ solar neutrinos and reactor neutrinos. This initial phase will allow us to debug the detector system and generate the first physics results from the **νEYE** experiment. Additionally, we are exploring the feasibility of adding elements to enable charged current interactions, which could further enhance our ability to probe neutrino properties.

- **LS** Phase (6-8 years)

Once the LS is installed in the target volume, we will prepare and deploy radioactive sources to initiate the sterile neutrino search. If IsoDAR is available, it will be the first underground

accelerator-assisted sterile neutrino search. Simultaneously, we will continue detecting solar and reactor neutrinos to refine our understanding of neutrino oscillations.

In parallel, we will conduct ongoing measurements of geo-neutrinos to study Earth’s internal composition and supernova neutrinos to probe astrophysical phenomena. These efforts will provide a comprehensive neutrino detection program, maximizing the physics reach of the **ν EYE** experiment.

- **$0\nu\beta\beta$** Phase (8 years and beyond)

To extend the physics potential of the **ν EYE** experiment, we will initiate the $0\nu\beta\beta$ search by loading an appropriate metal isotope into the liquid scintillator. This step will allow us to probe the Majorana nature of neutrinos and explore the neutrino mass hierarchy.

A construction and implementation timeline for all phases of the experiment, including LS installation, detector commissioning, and physics data collection, is outlined in Fig. 27.

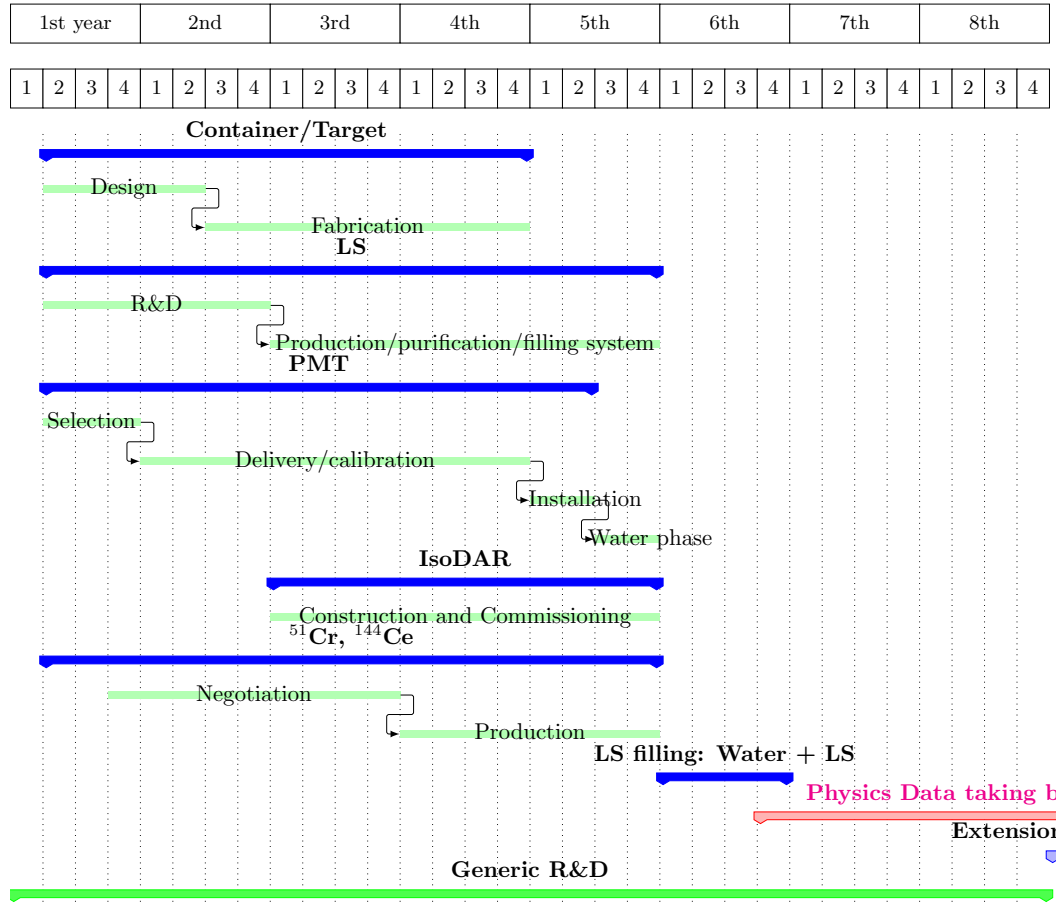


Figure 27: Our plan of the ν EYE experiment assuming 8 years of running the center. Note that as is explained above, we plan to have three phases of Water Cherenkov, LS, and $0\nu\beta\beta$ (beyond 8 years).